

The Measurement and Analysis of Drag Force on Moving Vehicle

Thesis is submitted in partial fulfilment of the requirements for the degree of

MASTER IN AUTOMOBILE ENGINEERING

SUBMITTED BY

SHARIQUE AHMAD

Examination Roll Number: M4AUT22008

Registration Number: 154341 of 2020-22

Under the guidance of:

Prof. (Dr.) NIPU MODAK

Department of Mechanical Engineering

Faculty of Engineering and Technology

Jadavpur University

Kolkata-700032

Faculty of Engineering and Technology
Department of Mechanical Engineering
Jadavpur University
Kolkata-700032

**DECLARATION OF ORIGINALITY AND COMPLIANCE OF
ACADEMIC ETHICS**

I hereby declare that this thesis contains literature survey and original research work by the undersigned candidate, as part of his Master of Automobile Engineering studies.

All information in this document have been obtained and presented accordance with academic rules and ethical conduct.

I also declare that as required by these rules and conduct, I have fully cited and referred all material and results that are not original to this work.

SHARIQUE AHMAD

Examination Roll Number: M4AUT22008

Registration Number: 154341 of 2020-22

**Thesis Title: The Measurement and Analysis of Drag Force on Moving
Vehicle**

Signature: *Sharique Ahmad*
.....
(Sharique Ahmad)

Dated: *04/07/2022*

Faculty of Engineering and Technology
Department of Mechanical Engineering
Jadavpur University
Kolkata-700032

CERTIFICATE OF APPROVAL

This forgoing thesis is hereby approved as a credible study of an engineering subject carried out and presented in a manner satisfactory to warrant its acceptance as a prerequisite to the degree for which it has been submitted, It is understood that by this approval the undersigned do not endorse or approve any statement made, opinion expressed or conclusion drawn therein but approve the thesis only for the purpose of which it has been submitted.

Committee on final examination for evaluation of the thesis

Signature:

Date:

Seal:

Signature:

Date:

Seal:

*Only in case, the thesis is approved.

Faculty of Engineering and Technology
Department of Mechanical Engineering
Jadavpur University
Kolkata-700032

CERTIFICATE OF SUPERVISION

We hereby recommend that the thesis presented by Mr. Sharique Ahmad entitled “**The Measurement and Analysis of Drag Force on Moving Vehicle**” was under our supervision and is accepted in partial fulfilment of the degree of Master of Automobile Engineering.

 04.07.2022

Prof. (Dr.) Nipu Modak
Thesis Advisor
Department of Mechanical Engineering
Jadavpur University
Kolkata

Professor

Dept. of Mechanical Engineering
Jadavpur University, Kolkata-32

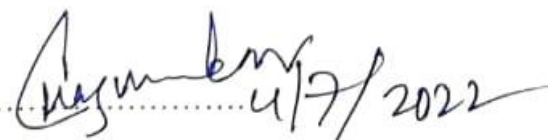
Countersigned by:

 04/07/22

(Head of the Department, Mechanical Engineering)

Date:
Dept. of Mechanical Engineering
Jadavpur University, Kolkata-32

Seal:

 4/7/2022

(Dean of Faculty of Engineering and Technology)

Date:
 DEAN
Faculty of Engineering & Technology
JADAVPUR UNIVERSITY
KOLKATA-700 032

Seal:

ACKNOWLEDGEMENT

I owe a great deal of gratitude to my highly respected thesis advisor Professor Dr. Nipu Modak of the Department of Mechanical Engineering at Jadavpur University for his exemplary leadership, priceless suggestions, continuous encouragement, and affection throughout the duration of the project, without which I would not have been able to complete this work. Working under his direction has been a privilege I'm proud to have had.

I would also like to express deep felt gratefulness to my friend Rajat Karn and Sagun Murmu for their kind support and guidance.

I would like to express my sincere appreciation to everyone of the lab staff at Jadavpur University's Mechanical Engineering department for their kind assistance, direction, and support throughout my entire project.

Additionally, I want to express my gratitude for the wonderful cooperation of all the non-teaching personnel, my entire batch, my seniors, and all of my junior friends.

Last but not least, I want to express my sincere appreciation and sentiments for my family, who have continuously provided me with the drive, motivation, and determination to pursue my academic goals.

TABLE OF CONTENTS

	PAGE NO.
DECLARATION	ii
CERTIFICATE OF APPROVAL	iii
CERTIFICATE OF SUPERVISION	iv
ACKNOWLEDGEMENT	v
TABLE OF CONTENTS	vi
LIST OF FIGURES	viii
ABSTRACT	x
1. INTRODUCTION	
1.1 Aerodynamics	1
1.2 History of Aerodynamic in cars	2
1.3 Drag	3
1.4 Drag coefficient	5
1.5 Lift coefficient	6
1.6 Background and purpose of the study	6
1.7 Aims and Objectives	9
1.8 Overview of the thesis	9
2. LITERATURE REVIEW	
2.1 Introduction	11
2.2 Outer design of different vehicles	11
2.2.1 Ahmed Model	12
2.2.2 Trucks	16
2.3 Some changes made throughout the road vehicles	18
3. METHODOLOGY	
3.1 Ansys	30

3.2 Ansys and CAD Theory	30
3.2.1 CAD design	30
3.2.2 Modelling	31
3.2.3 Meshing	31
3.2.3.1 Types of meshing models	32
3.2.4 Analysis	33
3.2.5 Results obtained through above method	34
4. RESULTS AND DISCUSSIONS	
4.1 CASE I- Comparison of cuboidal truck having sharp edges and cuboidal truck having circular edges.	36
4.2 CASE II- Comparison between Ahmed body having closed windows and Ahmed body with open windows.	43
4.3 CASE III- Comparison between Ahmed body and Ahmed body with blower at the top.	49
5. CONCLUSION AND FUTURE SCOPE OF WORK	
5.1 Conclusion	56
5.2 Future scope	57
6. REFERENCES	58

LIST OF FIGURES

	PAGE NO.
1. Figure 1.2(i):- Paul Jaray's vehicular top design.	2
2. Figure 1.2(ii):- optimized frontal area.	3
3. Figure 1.2(iii):- Mercedes-Benz CLA.	3
4. Figure 1.3:- formation of wake region and flow separation.	5
5. Figure 1.6(i):- Rolling resistance and drag relation with resistance force.	7
6. Figure 1.6(ii):- Flow visualization: (a) in a smoke filled wind tunnel, (b) through computer simulation.	8
7. Figure 2.2:- Different shapes of road vehicles.	12
8. Figure 2.2.1:- The 3D Ahmed vehicle model with dimensions in millimeters.	13
9. Figure 2.2.2(i):- 6 different case-studies of the towing trailer.	17
10. Figure 2.2.2(ii):- Pressure coeff. on the surfaces of the scale towing trailer.	18
11. Figure 2.3(i):- Orthogonal views of the body and dimensions.	18
12. Figure 2.3(ii):- Van model of the type of a reversed Ahmed model.	20
13. Figure 2.3(iii):- Computational Flow Domain.	20
14. Figure 2.3(iv):- Pathline velocity field at the rear part of the reverse Ahmed model with the upstream velocity, $U_o = 13.9\text{m/s}$	20
15. Figure 2.3(v):- Typical tourist coach.	21
16. Figure 2.3(vi):- Truck designs A and B used for simulation	22
17. Figure 2.3(vii):- Contour of static pressure	23
18. Figure 2.3(viii):- Velocity vectors behind the passenger car	23
19. Figure 2.3(ix):- Wake flow pattern of the Ahmed model.	23
20. Figure 2.3(x):- Wake visualization.	24
21. Figure 2.3(xi):- The bodywork shape of the automobile in the longitudinal middle section.	25
22. Figure 2.3(xii):- Sketch map of the slantwise angle variation of back windscreen.	25
23. Figure 2.3(xiii):- Typical CFD flow analysis for the lower part of a sedan car.	26
24. Figure 2.3(xiv):- Velocity and streamlines distribution on the car surface.	27
25. Figure 2.3(xv):- Optimized YF SONATA shape.	28
26. Figure 2.3(xvi):- Concept of design variables.	29

27. Figure 2.3(xvii):- Example of CFD simulation result.	29
28. Figure 3.2.3:- Inflation in boundary layer.	32
29. Figure 4.1(i):- Geometry used in ansys of cuboidal truck having sharp edges.	37
30. Figure 4.1(ii):- Geometry used in ansys of cuboidal truck having circular edges.	37
31. Figure 4.1(iii):- Named selection for both cases.	37
32. Figure 4.1(iv):-mesh of sharp edge truck.	38
33. Figure 4.1(v):-mesh of circular edge truck.	38
34. Figure 4.1(vi):- total pressure contour for sharp edge.	39
35. Figure 4.1(vii):- total pressure contour for circular edge.	39
36. Figure 4.1(viii):- velocity contour for sharp edge.	40
37. Figure 4.1(ix):- velocity contour for circular edge.	40
38. Figure 4.1(x):- velocity vector for sharp edge.	41
39. Figure 4.1(xi):- velocity vector for circular edge.	41
40. Figure 4.2(i):- Geometry of Ahmed body.	43
41. Figure 4.2(ii):- Geometry of Ahmed body with open windows.	43
42. Figure 4.2(iii):-Named selection for both the cases.	44
43. Figure 4.2(iv):- Mesh for Ahmed body.	44
44. Figure 4.2(v):- Mesh for Ahmed body with open windows.	44
45. Figure 4.2(vi):- Pressure contour for Ahmed body.	45
46. Figure 4.2(vii):- Pressure contour for Ahmed body with open windows.	45
47. Figure 4.2(viii):- Velocity contour for Ahmed body.	46
48. Figure 4.2(ix):- Velocity contour for Ahmed body with open windows.	46
49. Figure 4.2(x):- Velocity vector for Ahmed body.	47
50. Figure 4.2(xi):- Velocity vector for Ahmed body with open windows.	47
51. Figure 4.3(i):-Geometry of Ahmed body.	49
52. Figure 4.3(ii):-Geometry of Ahmed body with blower at its top.	49
53. Figure 4.3(iii):-Named selection for both the cases.	50
54. Figure 4.3(iv):- Mesh for Ahmed body.	50
55. Figure 4.3(v):-Mesh for Ahmed body with blower at its top.	50
56. Figure 4.3(vi):- Pressure contour of Ahmed body.	51
57. Figure 4.3(vii):-Pressure contour of Ahmed body with blower at its top.	51
58. Figure 4.3(viii):- Velocity contour for Ahmed body.	52
59. Figure 4.3(ix):-velocity contour for Ahmed body with blower at its top.	52
60. Figure 4.3(x):- Velocity vector for Ahmed body.	53
61. Figure 4.3(xi):-velocity vector for Ahmed body with blower at its top.	53

ABSTRACT

The price of fuel is rising at an alarming rate in this era of quickly dwindling natural resources. Because of the current fuel prices and the negative impacts of CO₂ and other emission gases on the environment, automakers all over the world are looking for innovative ways to make their vehicles more energy efficient and ecologically friendly. Improved aerodynamic vehicle designs that result in lower aerodynamic resistance forces and lower energy consumptions are one technique to accomplish this goal. These forces are highly relevant for any vehicle that can travel at a speed of 50 km/h or more, which includes virtually all passenger and commercial vehicles. Drag force is one of the primary barriers to achieving high speeds in a moving car. This study's major goal is to examine the drag coefficient and drag force values in various scenarios where the vehicle's design has changed or external equipment has been added to improve fuel efficiency. Using comparisons we can be able to know that which how we can get the optimum drag coefficient value. Using a three-dimensional Computational Fluid Dynamics (CFD) simulation in the Ansys programme, we look into techniques to lower the aerodynamic drag coefficient in this article. I made comparisons using the standard Ahmed model car body. Without any changes in the base design of the Ahmed model I compared it with some addition or say by just opening or closing the windows of the car. I have compared a cuboidal shape treating it as a truck having sharp edges while other with circular edges. To get a wide range of mesh cases for mesh optimization, ANSYS Meshing was employed. ANSYS Fluent software was also used to simulate all models. In order to compare these scenarios and investigate the model's aerodynamic behaviour, contours of velocity and pressure were used. In this I have used Standard K- epsilon method to simulate in ansys software. In this thesis I have mostly used same inlet and outlet condition for every case and also assumed the velocity of the wind 20m/s (72km/h) in every case. In this I tried to show that we can reduce drag coefficient by just changing the sharp edges to circular or curvy edges. It has been shown that using contemporary external aerodynamic add-on devices and making small structural changes to them significantly reduces the aerodynamic drag coefficient. At last, structural modifications are also employed and its effect on drag coefficient is studied.

1. INTRODUCTION

1.1 Aerodynamics

Aerodynamics is the study of science of the flow of gaseous fluids (like air) and the force acting upon bodies (such as automobiles) while in motion correlative to such fluids [1]. To compute the power and times through which it acts, it is critical to comprehend how air moves within the body. For this reason, space flow (the air around the body) velocity, pressure, and temperature are estimated as functions of position and time. Aerodynamics typically consists of two parts, mostly exterior and interior (ibid). External aerodynamics examples are such as aerodynamics aircraft, blades of wind turbines, rockets, and road vehicles. In the other way, internal aerodynamics is a flow study by using corridors on solid objects. Internal aerodynamics examples are such as jet engines pipelines and rocket engines. In this thesis, the work is mainly focused on the AHMED CAR as external aerodynamics with the judgement of SUV keeping in mind.

Aerodynamics is the scientific study of how any moving object interacts with the air. It examines how a body behaves when it comes into touch with the air and then calculates the forces that the air flowing over and around the body will exert. The most crucial elements influencing a car's performance are the air flowing over and around the body [2]. For example, driving the car as swimming through an endless ocean made of air. For the previous few years, it has been seen that there has been significant pressure on vehicle manufacturers to propose some workable solutions to move ahead of this dilemma since the air quality is deteriorating and there is a shortage of natural resources, particularly oil. In the past, the horsepower of the engine was crucial to maintaining the performance sector of high-speed cars. However, design experts nowadays are becoming accustomed to the idea of using aerodynamics to increase a vehicle's economy [3, 4]. It has been shown that gasoline accounts for around half of the vehicle's energy consumption due to aerodynamic drag [5, 6]. Therefore, it can said, drag reduction is the one of the major outlook to automotive manufacturers to be opt for. Implementation of shaping the vehicle body and addition of various add on devices come up with development for low drag, which may become a necessary part of the design process.

1.2 History of aerodynamic in cars

In starting of 1900s At first glance, they appeared to be copies of ships and aeroplanes. At first, engineers fail to recognise the ground effect and the loss of flow homogeneity; as a result, there is an increase in drag. They might have also overlooked the wheels because having them detached from the car's chassis distorts the flow. As a result, the wind resistance rises, making it impossible to distinguish all of the improvements made to the car's chassis as a whole.

Around 1920 – 1970 the first wind tunnel, used to enhance vehicle aerodynamics, was invented around this time. The purpose of the wind tunnel did not influence the aerodynamic forces. The goal was to decide on the vehicle configuration such that the power would only be reduced when necessary to take the car up to a specified speed. We have studied Paul Jaray's work since he was the first engineer to build an automobile while considering aerodynamics, and his designs were based on actual aerodynamics and airplanes. Buyers, however, did not like his designs. After a few years, other engineers began to incorporate his concepts into their designs [7].

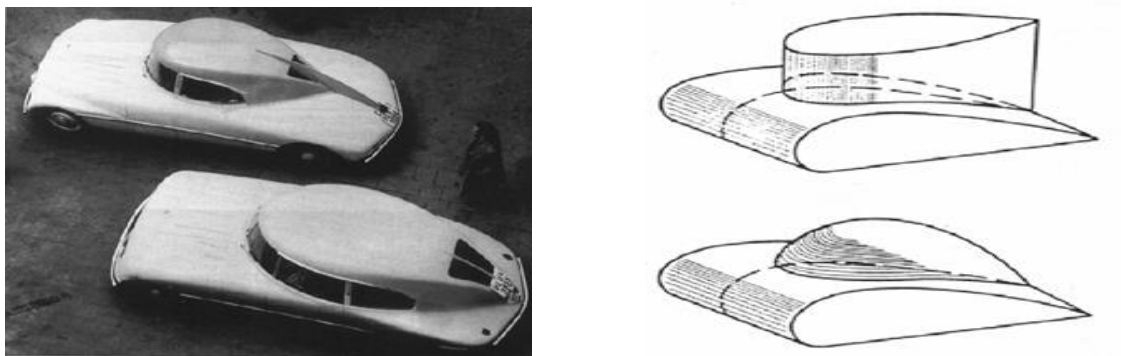


Figure 1.2(i)- paul jaray's vehicular top design

And from that point forward, the aerodynamics of the cars have started to have unexpected effects. As a result of the goal, the fuel consumption must decrease along with the drag resistance. There are essentially two methods for reducing drag resistance:[10]

- Reducing the frontal area, as the air impacts this area. So it helps to reduce drag resistance by lowering the frontal area.
- Reduce coefficient of drag (C_D) to improve aerodynamics.

Today, it is clear that the first choice is impractical. Each and every manufacturer has reached the same optimal equation –

$$A=0.81*(b*h)$$

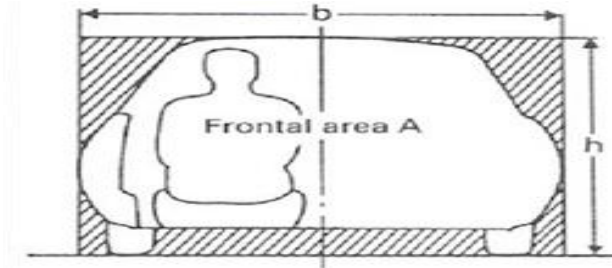


Figure 1.2(ii)-Optimized frontal area [11]

Efficiency is the main concept on people's minds these days, and designing a new car would be impossible without considering aerodynamics. For instance, in 2013 the most aerodynamic production car—the Mercedes-Benz CLA—made its debut. Its drag coefficient was (C_D) of 0.23 [12]. The improvement and optimization of the engine cover, front, mirrors, and other aspects led to the achievement of this drag coefficient number.



Figure 1.2(iii)-Mercedes-Benz CLA

1.3 Drag

In fluid dynamics, drag can be said as air resistance, it is quite like of friction of solid mechanics, or fluid resistance, another type of friction in the environment of fluid, is a force act on the opposite direction relative to a motion of an object moves with respect to a surrounding fluid. This drag can occurs and exist within two fluid layers as surfaces or between a fluid and a solid surface. Just like other resistive forces acts on the body, for example dry friction, mostly which do not depend on the velocity, but, the drag force depends

on velocity. Drag Force for the most parts, it depends on the velocity, frontal area, and most important also on the coefficient of drag of the body.

The drag force is expressed as:

$$F_D = \frac{1}{2} * C_D * \rho * A * V^2$$

Where,

F_D is drag force; ρ is density of fluid medium i.e. air; A is the frontal area of the body facing the fluid; V is the velocity of the body; C_D is the coefficient of drag of the body.

In a similar vein, lift force is a significant issue that design engineers must address because excessive lift can cause a vehicle to lose grip at high speeds, which could result in deadly injury to the driver and other pedestrians as well as damage to public property. Therefore, it is generally preferable to keep the lift in good condition and within the allowed range. The lift force is represented as follows:

$$F_L = \frac{1}{2} * C_L * \rho * A * V^2$$

Where,

F_L is the lift force; ρ is the density of fluid medium that is air; A is the frontal area of the body facing the fluid; V is the velocity of the body; C_L is the coefficient of lift of the body.

It can be seen from the equation of drag that drag force is proportional to the square of the speed which means it suggests that as body speed increases, air resistance grows exponentially [8]. According to the concept of fundamental fluid dynamics, flow separation control is one of the major interests from fluid dynamics [5, 9]. The size of the wake area is determined by the flow separation location and therefore, the amount of aerodynamic drag is also determined accordingly. If the air flows above the car separate at the rear, this is known as the wake, and it creates a significant low pressure turbulent region behind the vehicle. This wake contributes to the development of drag pressure. Researchers utilise a variety of strategies to manage this flow separation, either by preventing it or by lessening its effects.

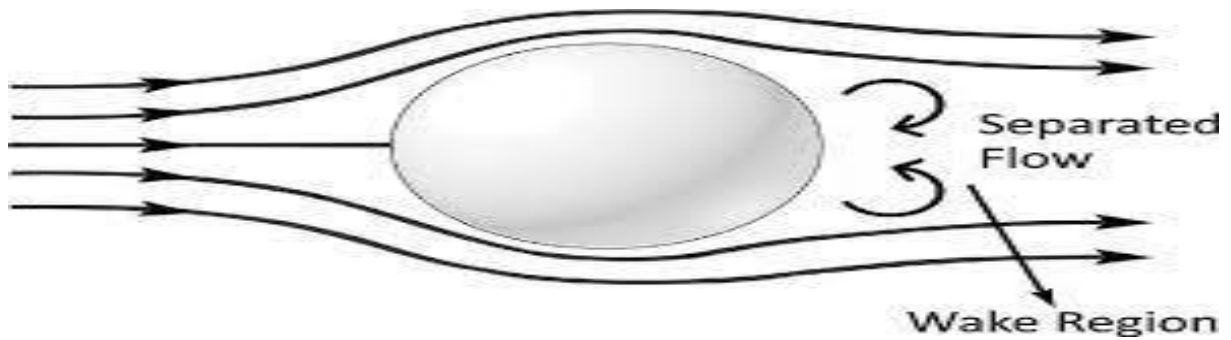







Figure 1.3- formation of wake region and flow separation

1.4 Drag coefficient

In fluid dynamics, the coefficient of drag is a dimensionless quantity used for quantifying the drag or resistance of an object undergone in a fluid environment; it can be either air or water. It has its significance used in the drag equation in which if a drag coefficient is lower it indicates that the object will have less drag in aerodynamically or hydro dynamically. The drag coefficient is always correlated with a certain or specific surface area.

NAME	SHAPE	DRAG COEFFICIENT VALUE(C_D)
Sphere		0.47
Half Sphere		0.42
Cone		0.50
Cube		1.05
Angled Cube		0.80





Long Cylinder		0.82
Short Cylinder		1.15
Streamlined body		0.04
Half Streamlined Body		0.09

Table 1.4:- Drag coefficient values of some structures

In the given following image, there are some examples of the Coefficient of Drag which depends on the shape of a vehicle. We can see the area of impact as well as the shapes of impact and these are very much important to reduce by reducing drag coefficient.

The equation will be:

$$C_D = F_D / ((1/2) * \rho * A * V^2)$$

Where, F_D is Drag Resistance

ρ is air density (1.225 kg/m³)

V is speed (m/s), A is projected area.

1.5 Lift coefficient

There is a lift coefficient as well as a drag coefficient. The lift coefficient is a value that has no dimensions. This coefficient is used to determine how much force the body receives from the flow incident on it in the transverse direction.

The lift coefficient can be expressed as the following equation:

$$C_L = F_L / ((1/2) * \rho * A * V^2)$$

Where, F_L is Lift resistance.

1.6 Background and purpose of the study

The continually rising demand for energy has its own direct effects on fuel costs. Therefore, these along with the environmental issues brought on by car exhaust gases are the main drivers behind the need to minimise road vehicles' fuel usage. Fuel consumption can be decreased and top speed can be increased with a decrease in aerodynamic drag [14]. Due to

the threat of global warming, designers are under pressure to improve vehicle designs through external modifications and add-on equipment [15]. In order to maximise performance and passenger comfort, the exterior car design has been changed. Aerodynamics affect the car's performance as well as its comfort and control [16]. Most of these advancements have concentrated on reducing drag coefficient in order to increase acceleration and fuel efficiency [17]. Road vehicle aerodynamics is one of the more complicated fields since it deals with how vehicles' contemporary, asymmetrical exterior designs interact with the road surface [18]. Heisler [19], Katz [20], Levin [21] and Schuetz [16] mentioned that Rolling resistance and aerodynamic drag significantly increase the resistance to vehicle movement as shown in Figure 1.6(i). When moving at a high speed, aerodynamic drag rises, but rolling resistance stays virtually constant. Aerodynamic drag and rolling resistance are equal at 65 km/h, but at speeds below that, rolling resistance is greater. As a result, at low speeds, aerodynamics is less significant.

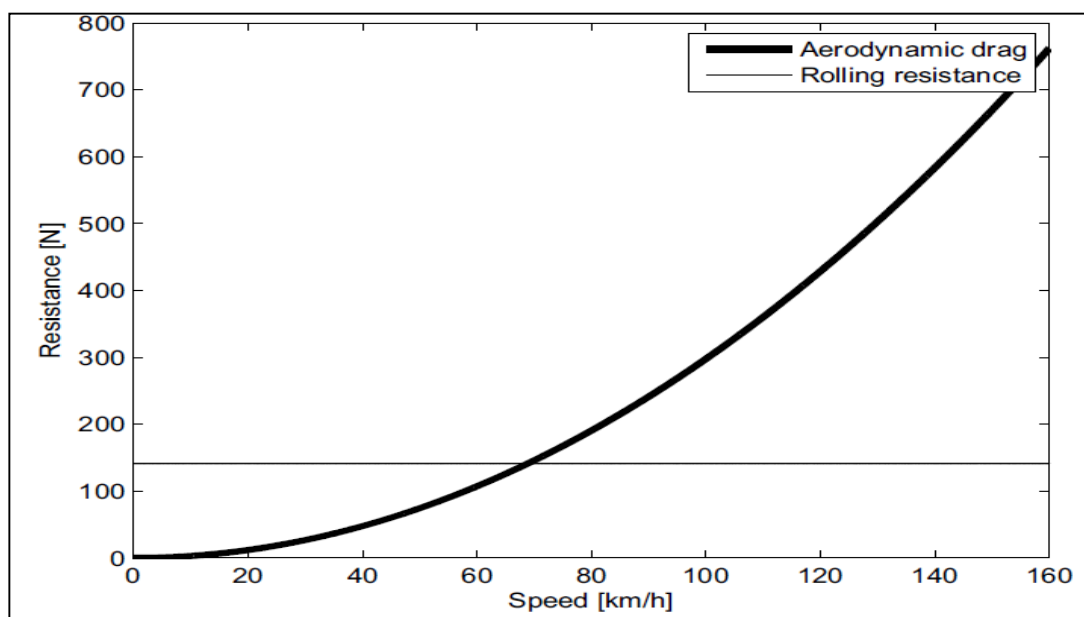


Figure 1.6 (i): Rolling resistance and drag relation with resistance force [9]

Hucho [22]; Krishnani [15] and Schuetz [16] illustrated Visibility, performance, cooling, comfort, drivability, and local forces are all included in a vehicle's aerodynamics. Aerodynamic behaviour is utilised to lower the drag coefficient, increase vehicle stability, particularly at high speeds, enhance the cooling of the engine and the brakes, and increase passenger comfort and visibility.

There are two basic methodologies, which can be utilised to investigate vehicle aerodynamics; these are Computational Fluid Dynamics (CFD) and experimental

observations. CFD is a subfield of fluid mechanics that employs numerical analysis to address a variety of issues involving fluid flows. High performance computers can be used to produce better numerical simulation. In contrast, an experimental approach is a process that uses observation to confirm or disprove a hypothesis. Vehicle aerodynamic behaviour has been experimentally studied in wind tunnels. There are restrictions on using the wind tunnel, though [16]:

1. In the studies using scale models, the Reynolds number is quite low.
2. It is challenging to include all automotive design features in scale models.
3. Due to the wind tunnel's limited limits, blocking effects occur.
4. Around the wind tunnel, turbulence and crosswinds are barely depicted.
5. Complete prototype testing is highly costly.

Because there were no real automobiles accessible at the commencement of the automotive industry, models supplied using numerical methods for assessment were used. The arguments for justifying the adoption of a numerical approach include the reduction in the development cycle, the reduction in expenses, and the increase in flexibility. Figure 1.6(ii) depicts the complexity of the smoke-enhanced flow around the car in the wind tunnel (a) and the air streamline produced by computer simulation for the vicinity of the wake [16]. It is obvious that the air flow over the car's roof is divided at the end of the roof; this phenomenon is referred to as the wake. The low pressure area that makes up the wake is behind the car [23]. The back of the car is fashioned in the appropriate manner since the wake is essentially crucial.

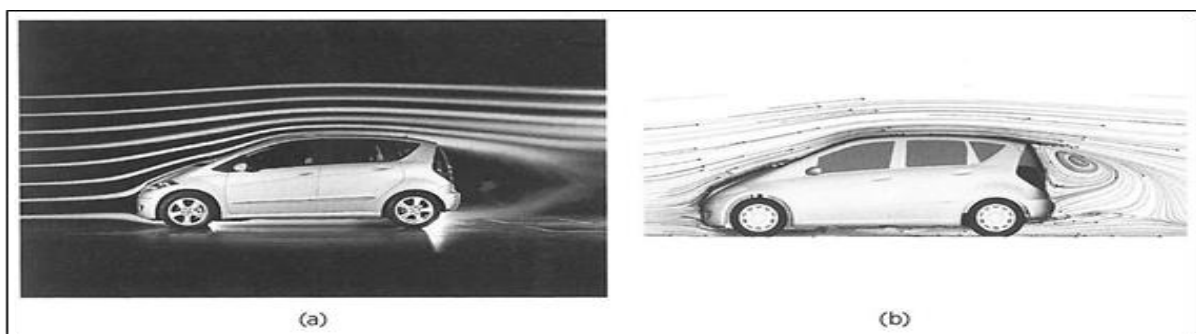


Figure 1.6(ii): Flow visualization: (a) in a smoke filled wind tunnel, (b) through computer simulation [16]

1.7 Aims and objectives

The aim of this present study on moving vehicle at high speed is focused on reducing drag coefficient of the vehicle moving with different speed and other parameters.

Simulation of this study is aimed to obtain aerodynamic forces, velocity contours and pressure contours acting on the moving vehicle. Thereby optimizing the required design criteria for the vehicle, and to reduce power consumption and increase in safety as well as stability of the ride.

The research objectives are:

1. Simulation of moving vehicle (Ahmed body) with sharp cornered design at given speed and to obtain its affecting aerodynamic parameters. Comparing it with between sharp edged vehicle (Ahmed body) with round edges.
2. To investigate the Simulation results for cases where 2 cases considered, one with moving Ahmed body with open window and other with Ahmed body with closed window, moving under same speed. To study the effects of drag forces and obtain the comparative results for provided criteria.
3. To study the effects of modified design , where a blower is attached to the top of the moving Ahmed body (aiming to generate power being provided to the vehicle), a comparative study of drag coefficient and power consumptions for cases with the blower and one without any blower on the top of the body.

1.8 Overview of this thesis

The thesis is organised as follows:

Chapter 1 is all about the basic introduction related to the aerodynamics. In this we go through the basics definition of the terms with there related expressions. Starting with the history for the aerodynamic design and then the research background and the motivation part and ending with aim and objectives of this work. The main purpose of this part is to just give a brief idea related to this work

Chapter 2 is wholly made for the literature review part and in this part different models like Ahmed model, truck etc. are explained related to previously published reports. This part helps

in knowing the gaps in previous studies and with this help it is explained. The main purpose of this part is to fill the gap related to the thesis work which was done earlier and with respect to this thesis.

Chapter 3 explains the methods used to do this study in which Ansys and CAD is explained briefly. How these simulation software help in getting the optimum results is described in this part by explaining each steps related to ansys software. In this part start from creating the geometry to meshing to analysis to lastly getting the results all these steps are explained one by one. The main purpose of this part is to know the use of software to achieve the required simulation work to get the final results like drag coefficient values, the different velocity and pressure contours etc.

Chapter 4 is fully dedicated to the results and discussions for the different conditions I have used it to compare the drag force and drag coefficients. In this part I have compared (on the basis of obtained results through the simulation work done with the help of chapter 3) different meshes, velocity contours, pressure contours and lastly the drag coefficient as well as drag force values to study the aerodynamics. In this part I have calculated some values using defined formulas to compare between different models.

Chapter 5 shows the conclusions and suggested future scope work following the present studies. The purpose of this part is to interpret the arguments and that could determine possible future studies.

2. Literature review

2.1 Introduction

This portion includes a survey of the literature on the aerodynamic behaviour of road vehicles. The goal is to offer background knowledge on two important topics. And These are in road vehicle aerodynamics, namely reduction of drag and vehicle stabilisation. The several exterior designs of road vehicles are described in the next section. concentrating on prior studies on-road vehicle models that is pertinent to the current investigation. Additionally, the implications of external design adjustments on streamlines, coefficient of drag and coefficient of lift are explored. An assessment of the influence of supplemental aerodynamic technology on the road vehicle is given, with an emphasis on the coefficient of drag and lift. Additionally, a critical analysis of earlier CFD modelling and experimental research. This article examines external design tweaks and gadgets that can enhance the general aerodynamic performance of road cars. A description of the flow around various automobile types, a study of additional aerodynamic additions and modifications utilised on road vehicles, and refinement of the aerodynamic characteristics of such car body are all covered.

2.2 Outer design of different vehicles

Can be seen in Figure 2.2 below, there are several various external styles for vehicles, and these are all quite sophisticated in terms of design [16, 22]. Road vehicles operate along the ground's surface (ibid). It is recommended that the outward appearance of the road vehicle be categorized into three in order to optimise the performance of cars. Furthermore, these subdivisions won't just be based on geometry; they'll also take into account the size, speed, and use of the vehicles. For instance, while the effectiveness of fuel expenditure is more crucial for large vehicles, the steadiness of speedy vehicles on the road during high speeds is more crucial (Obidi, 2014). Some modifications and aerodynamic devices are suitable for one category, such as cab side extender extensions which are suitable only for tractor-trailers.

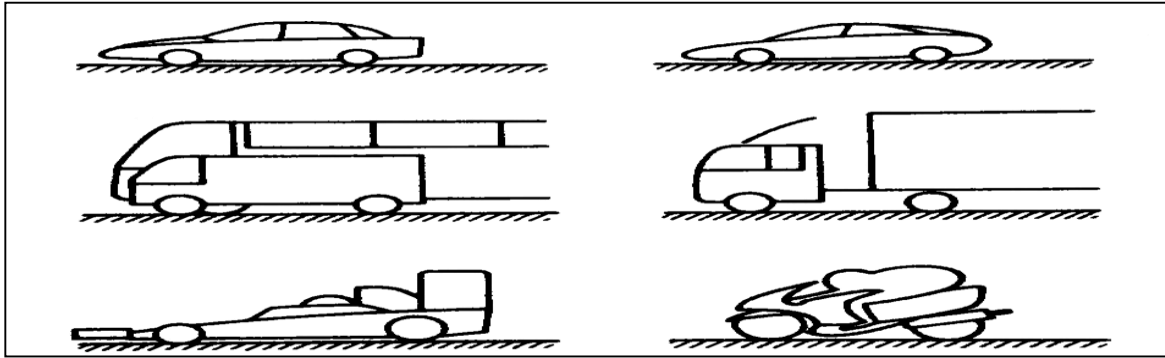


Figure 2.2: Different shapes of road vehicles [16]

2.2.1 Ahmed model

Ahmed model has been used in the study “Some salient features of the time- averaged ground vehicle wake in the study” [26, 27]. The Ahmed model is stated by author “simple and free from all kinds of accessories as well as wheels; nevertheless, it can be used to study the aerodynamic behaviour of a road vehicle based on the main features such as the slanting surfaces”. In the given Figure 2.2.1, it demonstrates as a full-scale, simplified, three-dimensional (3D) schematic of the Ahmed model, with primary dimensions. A plate under the design is marked by the red dotted line in the top view used by (Bello-Millán et al., 2016) like a new method to investigate and read the coefficient of drag. The authors stated, “the model is primarily designed to study the affect the slant angle (α) at the end part of the model on the drag coefficient and vortices behind the vehicle” [29, 30, 31]. These papers also describe, the statistical solutions are also validated using it. Grid convergence and turbulent models should be ensured for the simulation studies by assessing forces operating on the layout or measurements of the air velocity around the structure [28]. CFD was used for getting an accurate result with the simulation of airflow on and around the Ahmed model. In the published paper, it has stated, “many turbulent models have been investigated, specifically RANS [26, 29] and LES [32, 33, 34]”. LES results are very much accurate as RANS if they are compared to the experimental computations. The research shows the different changes would not be lies under the significance of the study enough as “it can justify very long simulation times in LES”.

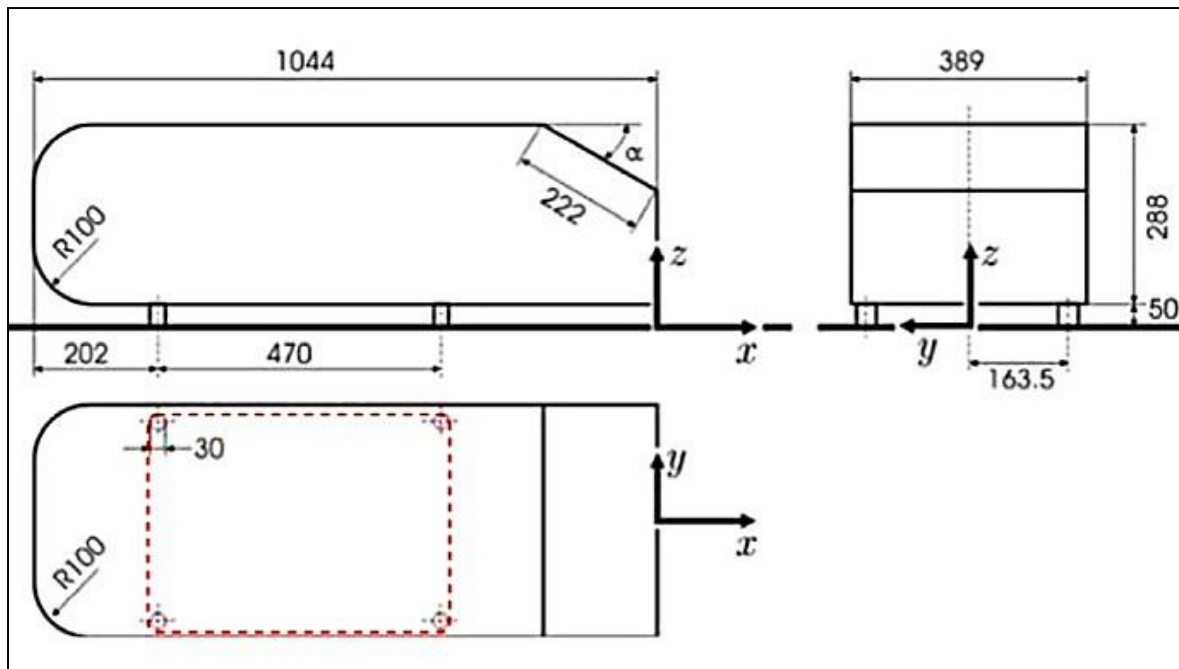


Figure 2.2.1: The 3D Ahmed vehicle model with dimensions in millimetres [28]

(Verzicco et al. 2002) [35] reveals that the Ahmed model is regarded as a proposed design for small vans, minibusses, and buses; however, the drawback of this type of specific pattern is that it is not just too limited to the front but also causes a significant issue at the tail due to the air streamlines being unable to return to previous form and “this is consistent with Lay’s study of 1933 [24]”. This is original reason behind sharp angles which were leading to air swirls behind the vehicle. Franck et al. [36] showed and stated, “numerically solved the unsteady airflow around the Ahmed model at a Reynolds number of 4.25 million. This study concentrated on the flow at the back of the Ahmed model (the wake zone). Two critical cases of the slant angle in this type of shape were 12.5° and 30° ” and it also stated by the author, “The slant surface length was fixed at 222mm for all cases and a tetrahedral mesh was used throughout the computational domain and the wedge layers were used in the model surfaces to get a better resolution for the body surface”. This is the most usable technique is currently usable by the researcher in the field of automobile.

In the paper “Computational study of flow around a simplified car body. Journal of wind engineering and industrial aerodynamics”, the author stated “the LES technique was used for the exploitation of the Smagorinsky Subgrid Scale Model, within which the flow within the wake zone can be in 2 completely different dimensions connected with a slant angle of lower than 12.5° and higher than 30° . But the flow within the wake zone is wide separated 3D with a slant angle between 12.5° and 30° . In general the mean drag coefficient (C_D) of this

numerical study was in line with the data gathered experimentally. The percentage relative errors were -1% for the finer mesh and +6% for the coarser mesh. This means that mesh size can affect the numerical results”. In the same paper named “Computational study of flow around a simplified car body. Journal of wind engineering and industrial aerodynamics” by (Guilmineau et al., 2008) stated, “numerically studies and investigated the result of the aerodynamic behaviour of the Ahmed model having two different slant angles of 25° and 35°” and 50% of the Ahmed model was in use within the governing equations, which had dimensions of 0.935 metres in width and 1.4 metres in height. It also stated, “the blockage ratio was 4.39% which depends on the computational domain dimension”. Therefore, the coefficient of drag was not accurate enough as we may have wanted. In the paper (Guilmineau et al., 2008), it has been stated, “the gap from the inlet side up to the initial position of the Ahmed model having two body lengths but from the end of the Ahmed model to the outlet side, there was three body lengths”. In the thesis paper, “Analysis of Novel Techniques of Drag Reduction and Stability Increase for Sport Utility Vehicles using Computational Fluid Dynamics”, it has stated, “two types of grid such as the first one was without stilts having total points of 1.8×10^6 with 16 blocks and the other one with stilts having a total no. of points of 3.6×10^6 with 32 blocks, were used and different turbulence models have been used since the Ahmed model with a slant angle of 25° can be thought-about a challenge case of turbulence modelling”. Then the paper also stated, “the simulations with different turbulence models may predict huge separation at the location with slant angle equal to 25° whereas the experimental studies show reattachment approximately half-way down the entire length of the slant face”.

(Conan et al., 2011) has stated in the paper named “Experimental aerodynamic study of a car-type bluff body. Experiments in Fluids”, “testing the drag coefficient of the Ahmed model having unlike values of slant angles and various measurement mechanisms”. A 3D Ahmed model was investigated by Howard and Pourquoiie [31] and they stated “ the slant angles between 12.5° and 30° causes high drag forces because of the low downwind pressure which is created behind the model”. The paper stated “ A combination of LES with a Spectral Vanishing Viscosity (SVV) technique was used to study the bluff body” studied by (Minguez et al.; 2008) and the approach that has been used is called as the LES-SVV method [27]. A study by (Watkins and Vino et el. ,2008) reveals two Ahmed model were experimentally investigated [37] with a change taken in consideration of the vehicle spacing. In his paper, he

stated “the researcher mainly focused on the formation of the wake causes behind the vehicle because of the drag force”.

A study by (Meile et al., 2011.) stated, “ the Ahmed model by using experimental and numerical approaches with two slant angles of 25° and 35° . They compared drag coefficient which were found by experimentally as a function of the Reynolds number. With the modelling results it has achieved using the ANSYS Fluent code”. In the study done by (Meile et al., 2011) they found the coefficient of drag to be decreased with increasing of Reynolds number and this was being confirmed by other researchers [28, 39]. Recently a study by(Bello- Millán et al., 2016) stated, “ the study using 55% scale model of the Ahmed model having a slant angle of 25° , but at different yaw angles, in a wind tunnel. The frontal projection area used in the experiments was calculated at 0 yaw angle, however, it is used for all scopes of yaw angles going through the study. A new method was added to calculate the coefficient of drag, placing a plate beneath the geometrical shape and attaching it to a force sensor (Figure 2.2.1)”. The coefficient of drag is obtained in terms of the Reynolds number. In this investigation, it has been seen that the result showed an increment of nearly or up to 30% as reported before. This gap is mainly because of the separation that has been generated at the edge, in the middle of the finish portion of the roof, and the initial position of slanting surface.

It came to the conclusion that the size of the model may affects the results. So, it is essential to inquiry the effect of the size of the model on the coefficient of drag. There are a number of on going study behind Ahmed model has done with the help both experimental as well as numerical way. But most of the studies mostly concentrated over the wake region which occurred beyond this type of shape. The study also see the effect made by slant angle over the wake. Quite a few ways of experimental-numerical were applied to calculate the coefficient of drag. But there are other studies that reveals applying aerodynamic devices. These are mostly useable for the decrement of the coefficient of drag on these types of geometric shapes. In accordance with our best knowledge, there are hardly work on the lift coefficient on Ahmed model. There is no report on the model scale, a report that might show that a plate is being used under the model. An upgraded scientific way was used to find out the coefficient of drag, but then again there are hardly analysis keeping the detail about of the effect of the dimension and configuration of the plates while obtaining coefficient of drag and coefficient of lift [28].

2.2.2 Trucks

A lot of fuel is consumed by the mix vehicles which are heavy. If we have to conquer aerodynamic drag during high speed, mostly, the power comes from engine as fuel is used, while the remaining is dissipated by rolling resistance through tyres, the resistance slope and, friction by drive train [40]. These losses were given first preference to be attended for an effort to boost growth fuel or energy miserliness of trucks. So, the primary concentration of these efforts are there wherever aerodynamics of the tractor acts and after the trailer. For that causes, all the studies have been handled the heavy or mix vehicle as united entity. The heavy vehicles have or have not highlighted the most areas are responsible for a rise in drag. In agreement with Hilmi Safuan [41], a truck's mass can have an impact on its engine load at low speeds, but when it picks up speed to 80 km/h or more, the truck's aerodynamics will have an impact on the engine load. The study states, “the information sympathizes with the studies of alternated researchers [19, 20, 21]. Since on the motorway, trucks are speeding upto approximately 100km/h, it is essential that aerodynamic enhancements are carried out to cut back operating prices”.

“The 1/7th scale livestock trailer model by aerodynamics and passive ventilation behaviour” was stated by Gilkeson et al. [42] using both experimental and numerical methods. The author also made their claim in the paper “An experimental and computational study of the aerodynamic and passive ventilation characteristics of small livestock trailers”, “refinement at the different level, a combination merge of structured hexahedral and unstructured tetrahedral cells was used”. The numerical findings were obtained using three distinct levels of mesh refinement, including 2.33, 3.14, and 4.65 million. And it has seen that almost in all instances y^+ values fell between 30 and 300 for all cases. Based on the typical frontal area utilised in the working portion, the blockage ratio was calculated to be 3.4%. Based on the combined length of the vehicle and trailer, the experimental work's air velocity in free-stream was 19.2 m/s, which is roughly equivalent to $Re = 1.74 \cdot 10^6$. Gambit (version 2.3.16) was used to build the mesh within the computational domain, and Fluent (version 6.3.26) was utilised to simulate every scenario.

In the computational models for the Spalart-Allmaras, realisable $k-\epsilon$ and SST $k-\omega$ models, three turbulent models were applied. The turbulence intensity tunnel was recorded at 2.65 percent at the wind intake. In the simulation studies, the authors applied the very same turbulence intensity. All walls have been given standard wall characteristics with no-slip

boundary criteria. In this study, author stated, “Six different case of the towing vehicle–trailer were used with a range of normalized heights (h/H) between 0 and 0.5” as shown in Figure 2.2.2(i). Pickup trucks and SUVs had wholly distinct proportions for towing automobiles. The resultant agreement between SST $k-\omega$ and realizable $k-\epsilon$ was good. The coefficient of drag from Spalart-Allmaras using an identical range of cells, however, was greater than turbulent models. Applying RANS models, as reported by many researchers and other publications [26, 29], one may predict the coefficient of drag of road vehicles with high accuracy. The statistical findings of several RANS models should be examined with the practical observations in order to choose an appropriate turbulence model for a given configuration. It is crucial to note that ventilating properties were essentially the same as all other towing vehicle elevations. When the trailer's rear end was excluded, there was strong agreement between both the analytical and simulation data and the results. After studying the effects of the carriage surface pressures, a location length was evaluated. The implications of the space between the trailer and the vehicle have still not been researched. Figure 2.2.2(ii) illustrates the coefficient of pressure on the scale towing vehicle-surfaces trailers as a result of the preliminary study.

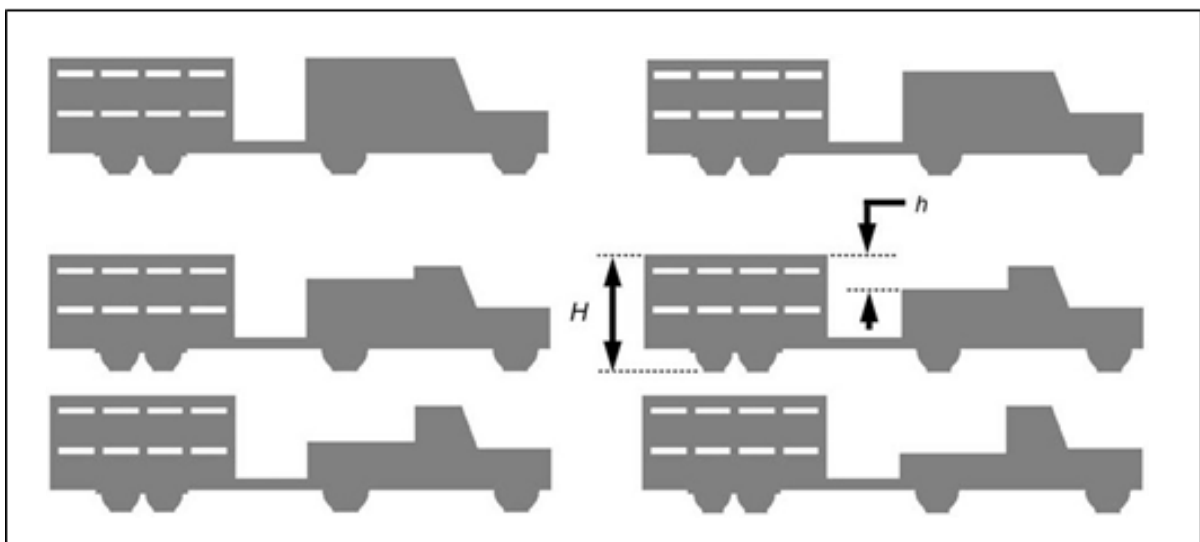


Figure 2.2.2(i): 6 different case-studies of the towing trailer [42]

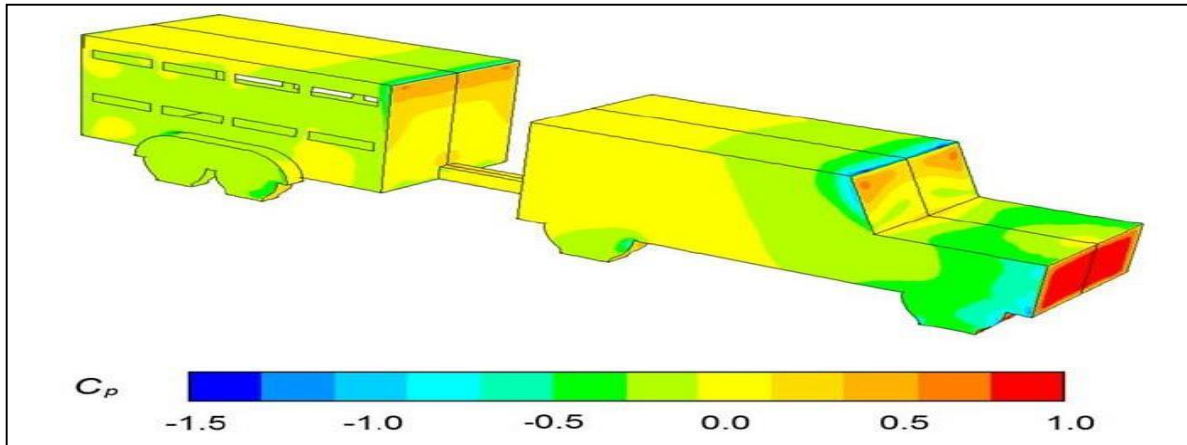


Figure 2.2.2(ii): Pressure coeff. on the surfaces of the scale towing trailer [42]

2.3 Some changes made throughout the road vehicles

Thacker et al. [39] and Verzicco et al. [35] both used experimental methods to study the approach of changing the shape of the Ahmed model from one with sharp edges to one with very soft edges. The air streamline was softer than that associated with the normal kind, which was known to cause a minimal reduction in air resistance and noise (the Ahmed model with sharp edges). As illustrated in Figure 2.3(i), Verzicco et al. [35] employed the LES model to assess the Ahmed model with one stilt to support this requirement. To attain mesh quality, one aerofoil-style stilt rather than four cylinder-style legs was used.

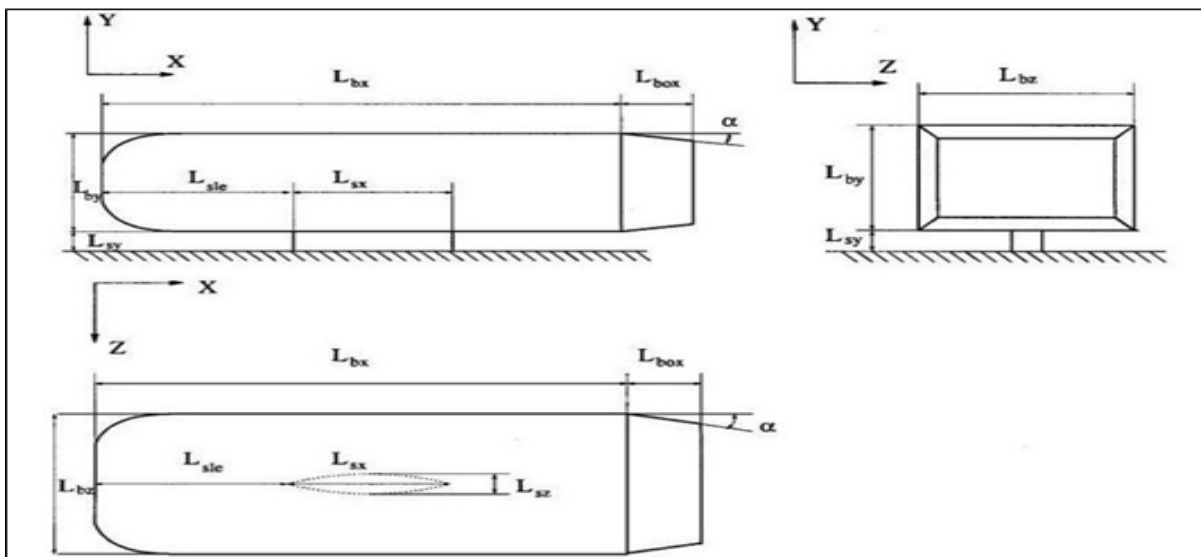


Figure 2.3(i): Orthogonal views of the body and dimensions [35]

A study was done by (Harinaldi et al. 2012) [44] studied 2 models with a reversed Ahmed model (with an opposite direction of airflow), as shown in the below Figure 2.3(ii). “The

model used in this study having the ratio of the size is relative to the original Ahmed model is a quarter with a front slant angle ($\alpha = 35^\circ$). It is postulated that the results from this study cannot be compared with the standard quality Ahmed model results because of the differences in model size and air direction” and the Figure 2.3(iii) shows the scientific way domain that was used during the study of simulation. Similar to what was shown in earlier research [29, 36, 45, 46], the computational domain size in this investigation is appropriate for producing accurate results. It also states, “The uniform velocity was 13.9m/s at the inlet and the velocity at the suction was 1m/s”. While the second type actively managed flow through suction, the first model had no flow control (Figure 2.3(iv)). This method was intended to increase the effectiveness of aerodynamic drag. According to Figures 2.3(ii) and 2.3(iv), the suction was achieved by employing a reduced flow rate and setting the suction velocity to 1 m/s (b).

This study is an combination of experimental and computational work. The properties of the flow field and drag forces were determined using the commercial solver ANSYS Fluent (version 6.3) using a traditional k-flow turbulence model computational technique. The experimental approach employed the controlled low speed wind tunnel to verify the reduction in aerodynamic drag found through calculations. Studies were done on how to make the vehicle more stable while using less fuel. By altering the flow separation, the swirls surrounding the model of the family vehicle were diminished. Using this method, the wake and vortex formation were diminished. The aerodynamic drag was on the verge of being decreased empirically by roughly 16.32 percent and 13.86 percent from a computational standpoint. The pathline of the velocity field at the back of the reversed Ahmed model is depicted in Figure 2.3(iv). Active flow control's (the pump's) power usage was not investigated. As a result, the drag coefficient reduction was inaccurate. The base bleed and this kind of adjustment are relatively comparable.

The sharp edges of the shape of the boxy body was changed to form soft edges by the designers and therefore, this method was helpful to lead to the softer air streamline reduces air resistance and noise more than the conventional version[35]. We can see in the given Figure 2.3(v), It displays a coach with a contemporary design, and the model also exhibits a streamline shape from all angles, including the coach's front, roof, and sides [47].

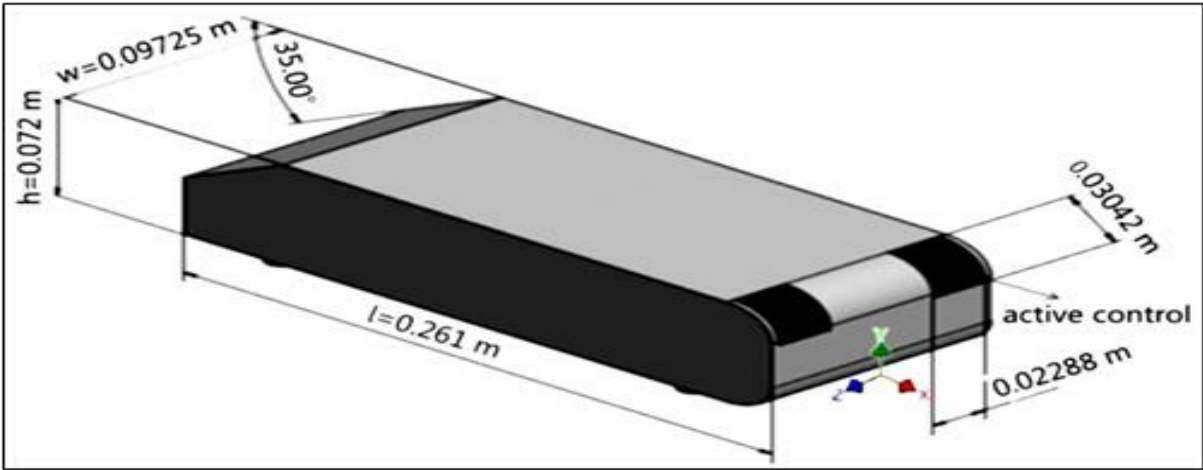


Figure 2.3(ii): Van model of the type of a reversed Ahmed model [44]

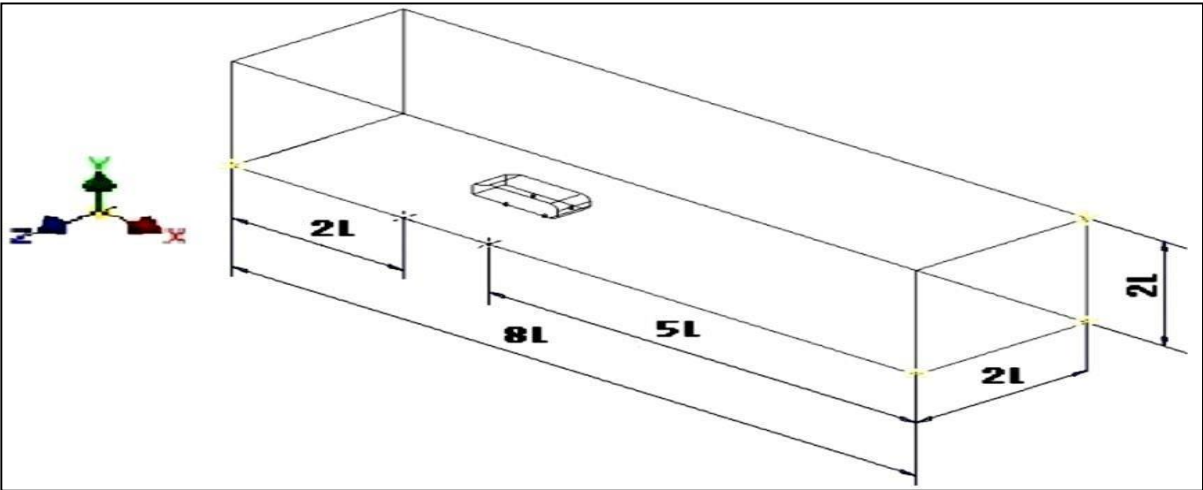


Figure 2.3(iii): Computational Flow Domain [44]

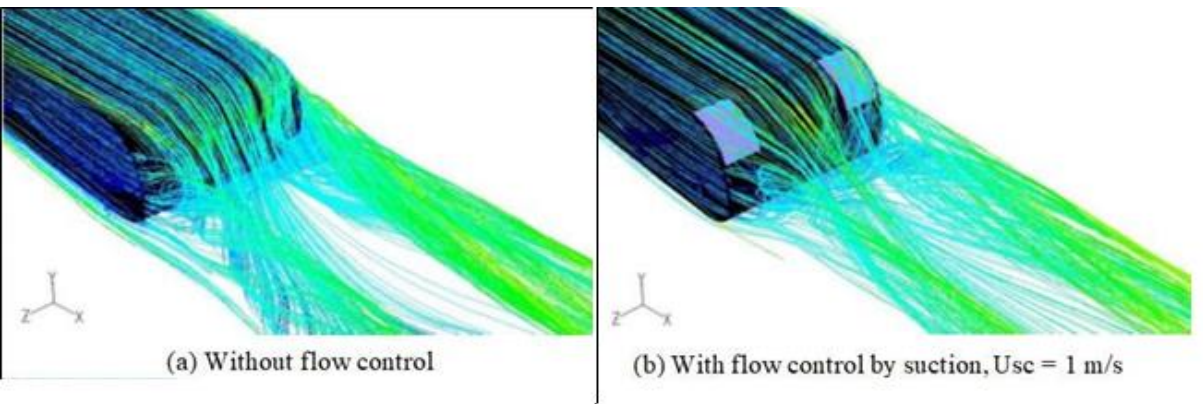


Figure 2.3(iv): Pathline velocity field at the rear part of the reversed Ahmed model with the upstream velocity, $U_0 = 13.9$ m/s [44]

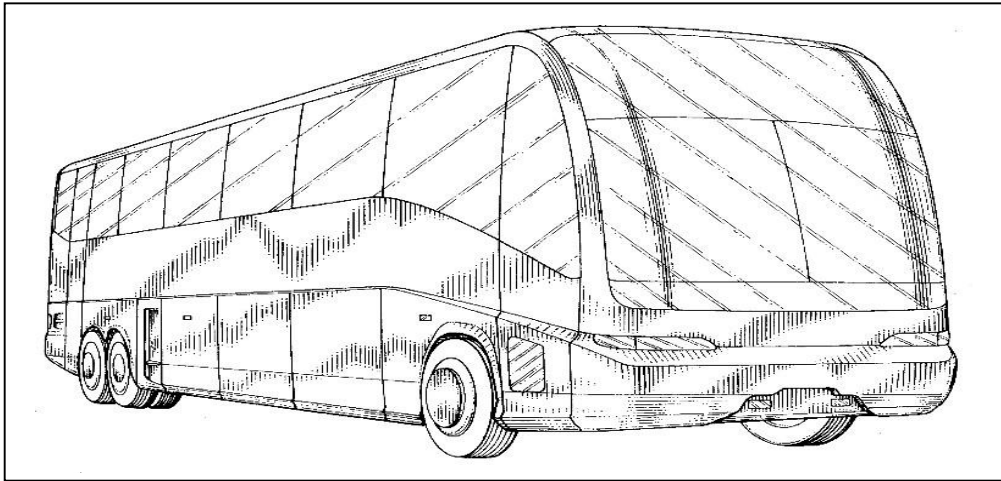


Figure 2.3(v): Typical tourist coach [47]

Roy and Srinivasan conducted research on the impact of aerodynamic drag and crosswind on truck fuel consumption [48]. The characteristics of the air surrounding a truck are remarkably similar to those of the bluff body, which was examined in order to reduce roadside accidents caused by wind loading and increase fuel efficiency. As can be seen, CFD was used to accomplish the task of analysing fluid flow in three dimensions and calculating the pressure distribution on the truck's exterior surface. The unstable fluid flow distribution was computed using the Navier-Stokes equation and a two-equation k -turbulence closure model. The work gives a hint as to whether it could be possible to simulate the aerodynamics of road cars using the k -turbulence model. The study was conducted underneath two vehicles using two distinct form designs and boundary circumstances. According to the study, the first boundary condition was a crosswind-free environment, and the second condition was a crosswind that was moderate.

“The computational area was of $40 l \times 10 d$, where l was the length of the truck and d was the maximum width of the truck is having. It is the worthiness of mentioning that the domain dimension in computational in this study was very large compared to the other numerical studies [29, 36, 45, 46] that has done”. Two truck designs—A (regular design) and B (modified design)—shown in Figure 2.3(vi) are used for simulation. It was noted that altering the truck's design may significantly increase the efficiency of its fuel consumption; as a result, this study [48] projected that 35 percent of the gasoline could be saved. As a result, the researchers demonstrated and established that altering a vehicle's external design can reduce its coefficient of drag.

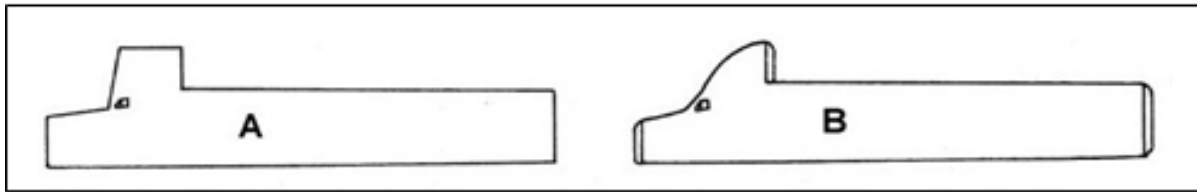


Figure 2.3(vi): Truck designs A and B used for simulation [48]

Some studies employed two-dimensional (2D) geometric vehicle works to expertly analyse the aerodynamic behaviour [43, 49, 50]. According to Ghani [50], some vehicles with 2D geometry may forecast the coefficient of drag despite having an inaccuracy of around 5%. Amirnordin et al. [49] modelled the two-dimensional geometry of a trailing vehicle in agreement with a hatchback-style passenger automobile and the pressure contour depicted in Figure 2.3(vii). According to Figure 2.3(viii), the hatchback car was creating counter-rotating vortices at the rear end that were comparable to those produced by the bus. The high pressure that exists at the front of the body had an impact on the structure of the wake in the back. The first imitation of aerodynamic behaviour is provided by this research.

The influence of the slant angle at the back of the vehicle owing to coefficient of drag has been widely investigated in the past couple years [25, 30, 31] since the airflow upon such road vehicle is really quite noteworthy than the airflow underneath the body [51]. The airflow performance at the backend of the three-dimensional Ahmed model has been examined in the given Figures 2.3(ix) [51] and 2.3(x) [52]. Due to the posterior part of the Ahmed Model's roof, which is portrayed by the illusion of a square back baseline, leading vortices that have been depicted in Figure 2.3(ix) and that were formed at its laterally borders that are considered to be actual pillars have been identified. There are no longitudinal vortices emerging from lateral edges just at rear of the vehicle in the analysis of two-dimensional geometries. The neglect of the third dimension is primarily responsible for the lateral boundaries being visible. Figure 2.3(x) depicts how well the side boundaries affect the wake formation as it operates in the 3D Ahmed model. In contrast to the three-dimensional geometry, the two-dimensional wake structural shape (as seen in Figure 2.3(viii)) (as in Figures 2.3(ix) and 2.3(x)). Thus it is hypothesised that on the symmetry plane, the outcomes from the 2D and 3D vehicles are equivalent.

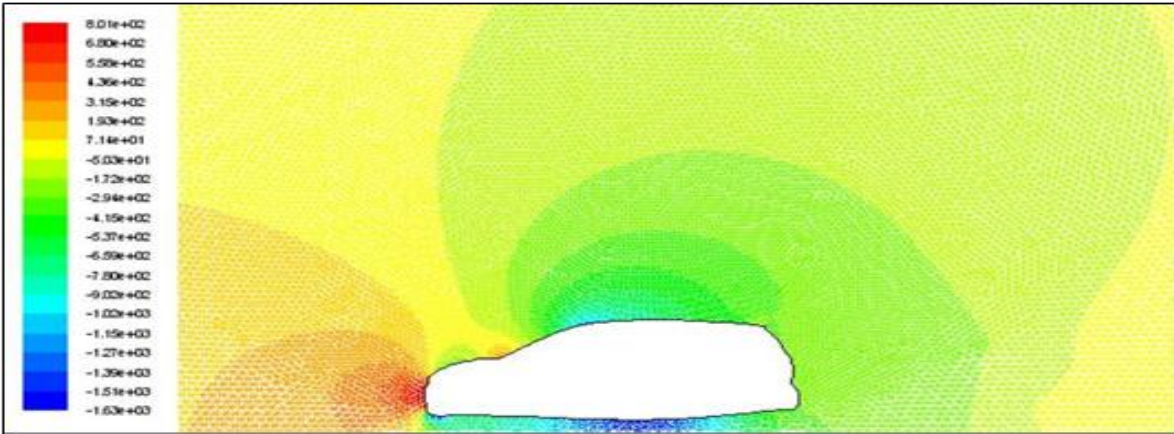


Figure 2.3(vii): Contour of static pressure [49]

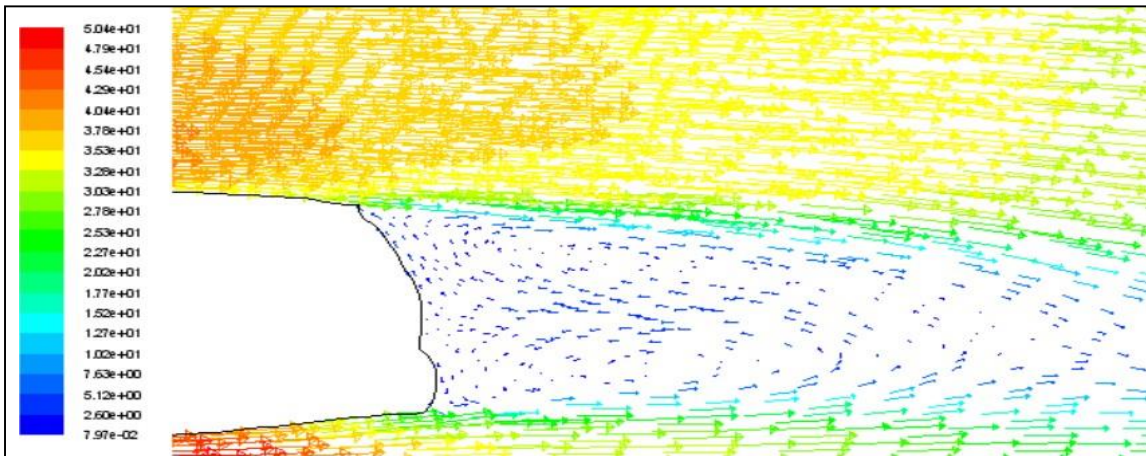


Figure 2.3(viii): Velocity vectors behind the passenger car [49]

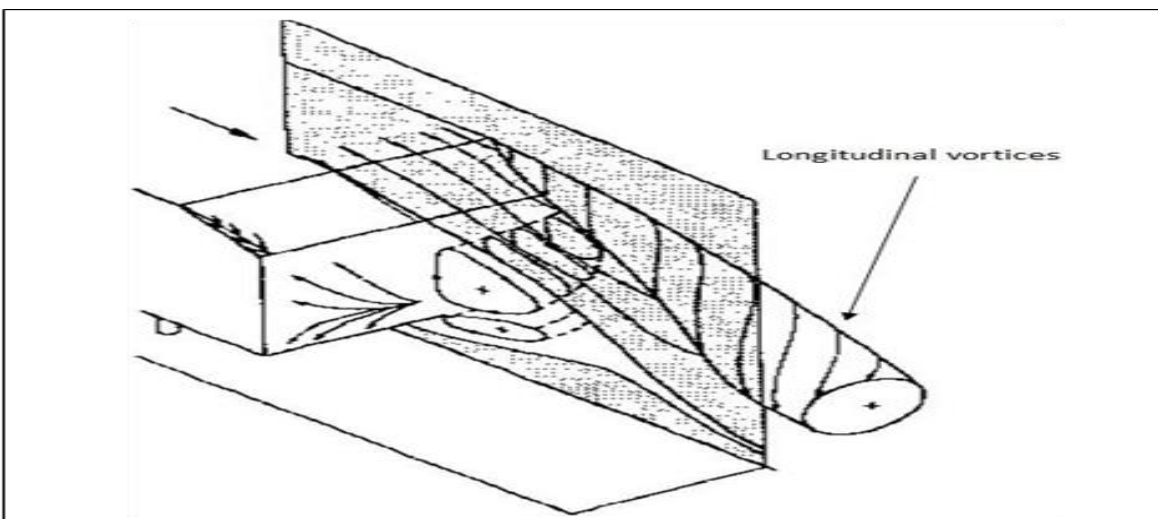


Figure 2.3(ix): Wake flow pattern of the Ahmed model [51]

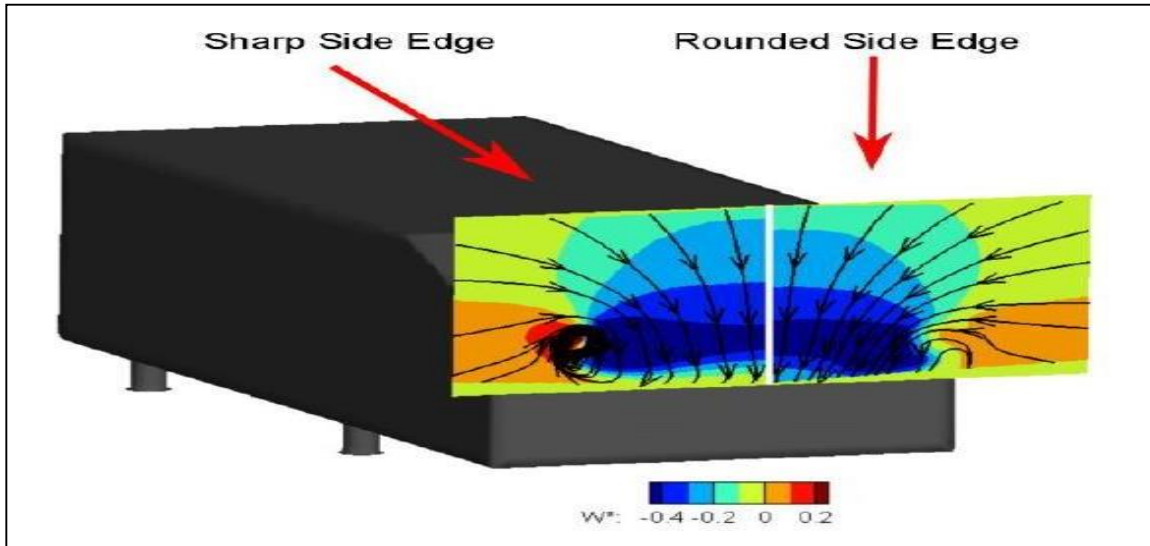


Figure 2.3(x): Wake visualization [52]

Guo et al. [43] used the finite element model in the form of two dimensional to analyse how a saloon car behaves aerodynamically. For modelling and analysis throughout the knowledge of the saloon vehicle model, ANSYS software was mostly employed. The saloon car's aerodynamic behaviour has been expressed for this purpose using the Navier-Stokes equations and our existing potential fluid theory equations. To achieve these as shown in Figure 2.3(xi), a simple model of car was modified to the front surfaces. It shows that, there's an assumption of having body of flat surface at the bottom of the saloon car. Here, some things were neglected in the modelling such as wheels, gaps of air and rear focus mirrors in order to simplify the solution in the modelling of finite element. Three different slantwise angles were employed at the back windscreen for $= 17^\circ$, $= 23^\circ$, and $= 30^\circ$, respectively, as shown in Figure 2.3(xii). In this example, the initial velocity of the air was 32m/s. The study was also conducted for four saloon automobile types with various car tails, including distributor-installed back, step-back, straight-back, and fast-back.

This investigation and additional experiments [35, 39, 48] supported the idea that external design changes could increase the drag coefficient. The k- turbulence model was the adapting mode for a computation of turbulent flow example. According to research cited in previous publications (Amirnordin et al., 2010), (Guo et al., 2011), (Harinaldi et al.;2012), (Levin and Rigdal et al.2011), (Miralbes et al., 2012), (Roy and Srinivasan et al. 2000), the k-turbulence model can be used to simulate the aerodynamics of road vehicles. The saloon car's velocity profile and air pressure distribution were examined in the study. The findings showed that the top and bottom surfaces of the car were subjected to intense pressure. There's an occurrence

of wind swirlin behind the car and that was depending on the car shape. The dragging and lifting force is influenced by the windscreen's rear's angle of inclination. Therefore, it can be said that increasing the angle of inclination of the rear can lead to increasing air resistance however decreasing lift force.

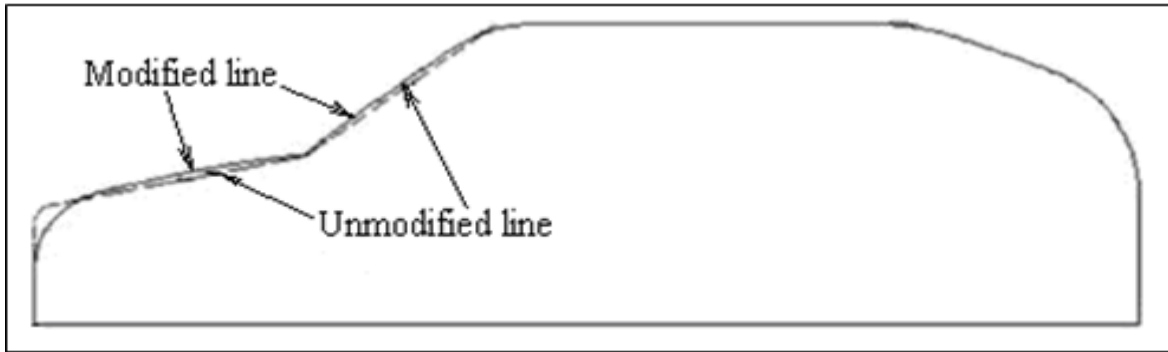


Figure 2.3(xi): The bodywork shape of the automobile in the longitudinal middle section [43]

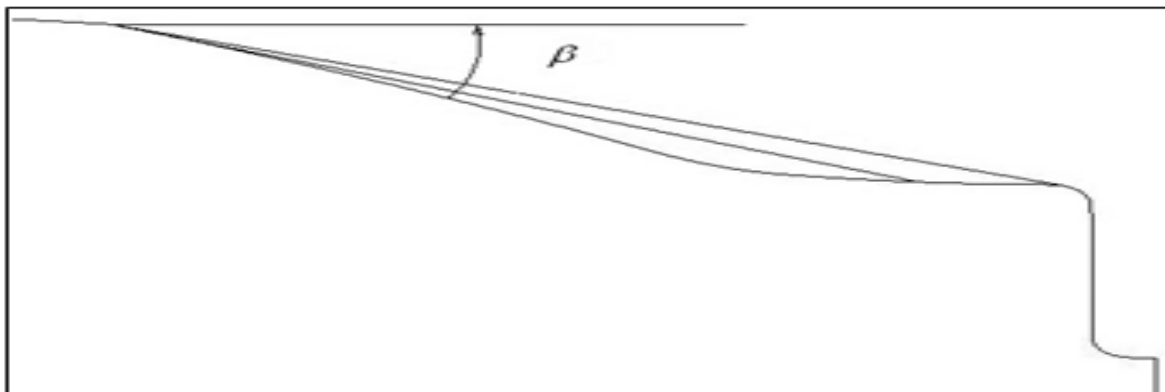


Figure 2.3(xii): Sketch map of the slantwise angle variation of back windscreen [43]

Barbut and Negrus presented a paper “CFD analysis for road vehicles-case study” [54] stated that noted that the lower section design of sedan automobiles had an impact on the air resistance, as seen in Figure 2.3(xiii). It has been stated that, the aerodynamic drag can be reduced to approximately 20% by re-designing the sedan’s car lower body. It is mainly due to the saloon car's fluid interaction with the automotive standard bluff body flow pattern and viscous effects. Computational fluid dynamics was used to optimize the design of the sedan car's lower part. For the use of CFD code, the parallel version of DxUNSp was used.

For the study of re-designing of the sedan car some things were kept in mind i.e., all-embracing size of a geometry with fixed inside components, and with a frozen geometry for the course of the wheels. Additionally, the target was conjointly to enhance aerodynamic drag while at the identical timetable, different vigorous characteristics were supposed to be

maintained as an example, stability. The authors stated, “a collection of global data for the basic reference. It was as follows: Reference speed was 25m/s, the reference Reynolds number was 2.5×10^6 , length was 1.5 m, total reference drag was 0.2411, and reference lift was 0.5662. There was a software called as MeTHIs software which was used to divide the usable computational domain into 8 domains and the code that runs the URANS version for getting an explicit time integration algorithm”.

There is also a software named as TecPlot software, which is used to display the results of some parameters such as velocity and streamlines of the research carried out before in the Figure 2.3(xiv). It was challenging to search for real conditions in wind tunnels. But it was carried out by the analysis of the flow beneath the sedan car has been done using computational fluid dynamics (CFD). Therefore, CFD is used as a tool and approached for analysis of the flow beneath the sedan car with the help of potential to establish significant changes, which is mainly for the best strategy in the auto industry. Therefore, in the paper study by (Barbut, D. and E.M. Negrus; 2011), “simulations show aerodynamic drag reduction from 0.2411 to 0.2105 which is almost 12.7% under the re-designing of the sedan car’s beneath body” [54].

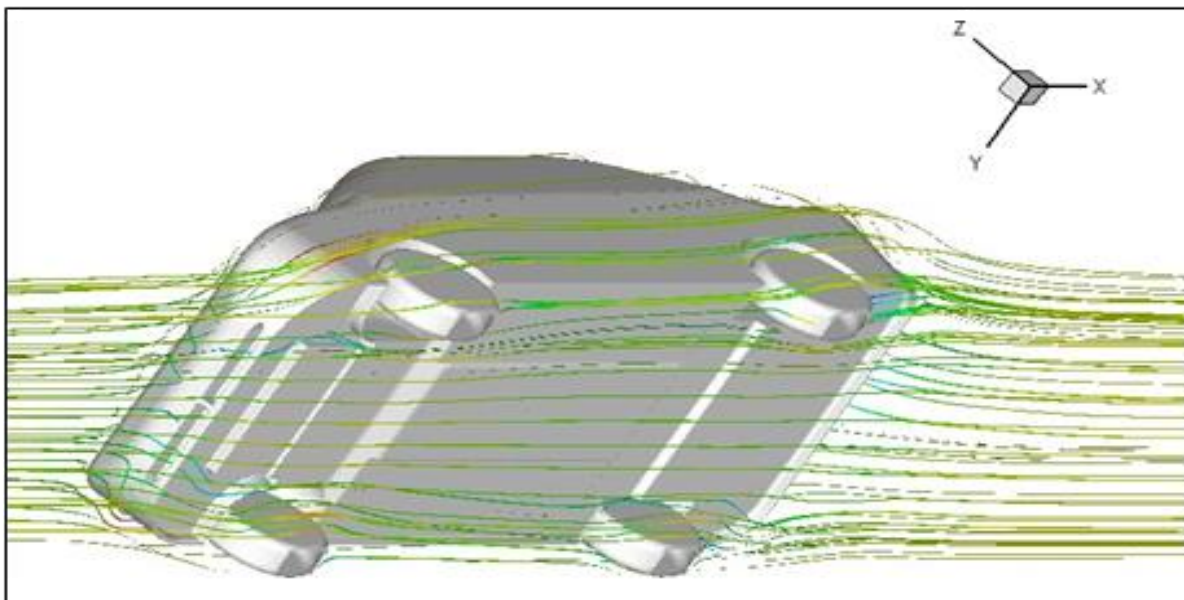


Figure 2.3(xiii): Typical CFD flow analysis for the lower part of a sedan car [54]

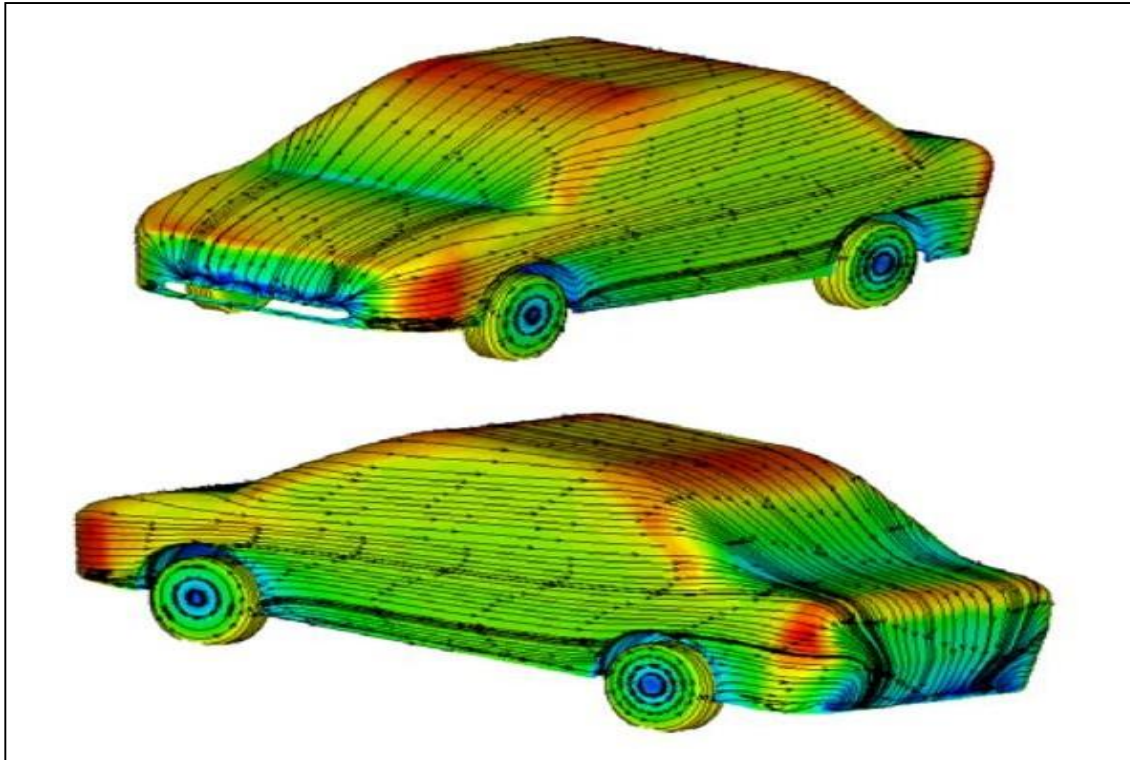


Figure 2.3(xiv): Velocity and streamlines distribution on the car surface [54]

A paper named “Aerodynamic design optimization of rear body shapes of a sedan for drag reduction” states the superficial design of a sedan car was optimized by using an ANN (Artificial Neural Network) (Song et al., 2012). Here, in this context, the authors were concentrated on the revision of the sedan car's rear peripheral design using only a modification up to the boot. The study by (Song et al., 2012) also stated that the rear side and the rear undercover were about to be optimized rear shape of the YF SONATA model as shown in Figure 2.3(xv). In order to prevent variations from the car's original design, there were two alterations made to each and every section. These adjustments included limiting the length and angle, as seen in Figure 2.3(xvi). The central emphasis of the mission was to reduce the readings of coefficient of lift (CL) and coefficient of drag (CD) to levels below those obtained from the baseline. The unstable fluid flow that arises around an automobile when it is travelling at a high speed was also examined using CFD.

In this paper (Song et al., 2012), the study's predictions of the pressure that is developed around over a sedan automobile as well as how the pressure evolves as per drag coefficient have also been seen. That has the best detection result when compared to the experimental data, the DES model, which is based on the $k-\epsilon$ model, was chosen [55]. Half of the YF SONATA's geometry was inspected to curtail on simulation time, and GAMBIT and Tgrid

were deployed to develop meshes. Here, three boundary conditions were taken in to the consideration such as –

- (i) Airflow was from the front portion of the car with a rate of 100km/h,
- (ii) The automobile's wheels revolving at a speed of 84.175 rad/s, or 100 km/h. and,
- (iii) The surface circumstances with a pace of 100km/h.

And as the outcome result was expected, it shows DES is preferred over RANS and LES. Just like in Figure 2.3(xvii), it displays a CFD simulation scenario with having results from 46 cases that are equivalent to the test set. In the study by (Song et al., 2012) reveals the experimental evaluation, 1/4th scale model of YF SONATA has been used and tested in a wind tunnel experiment at the Korean Air Force Academy.

“The full-size model of the YF SONATA was tested in the Hyundai Motors Corporation wind tunnel to confirm the active effect of an air flap on the aerodynamic performance. The full-sized experimental study showed that the aerodynamic performance was improved by approximately 7.1% if the intake of the engine room was closed by an air flap. The theoretical and experimental studies for a normal design show that the YF SONATA’s CD was 0.31 at 100km/h but for the intake-closed model reduced the CD to 0.263~0.279”. The authors [55] showed the coefficient of drag (CD) which stated “the average of CD over five seconds was 0.266 which was taken as the base value in this research. Immediately after the moving car, fluctuations in the CD occur until about 2.3 s. Therefore, an unsteady phenomenon can be observed”.

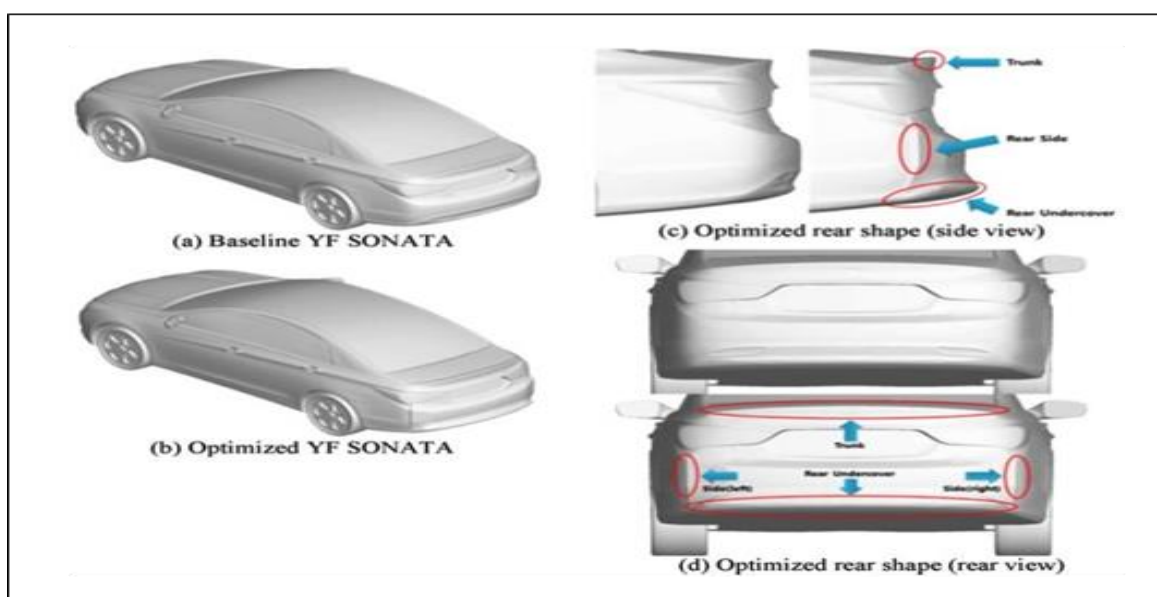


Figure 2.3(xv): Optimized YF SONATA shape [55]

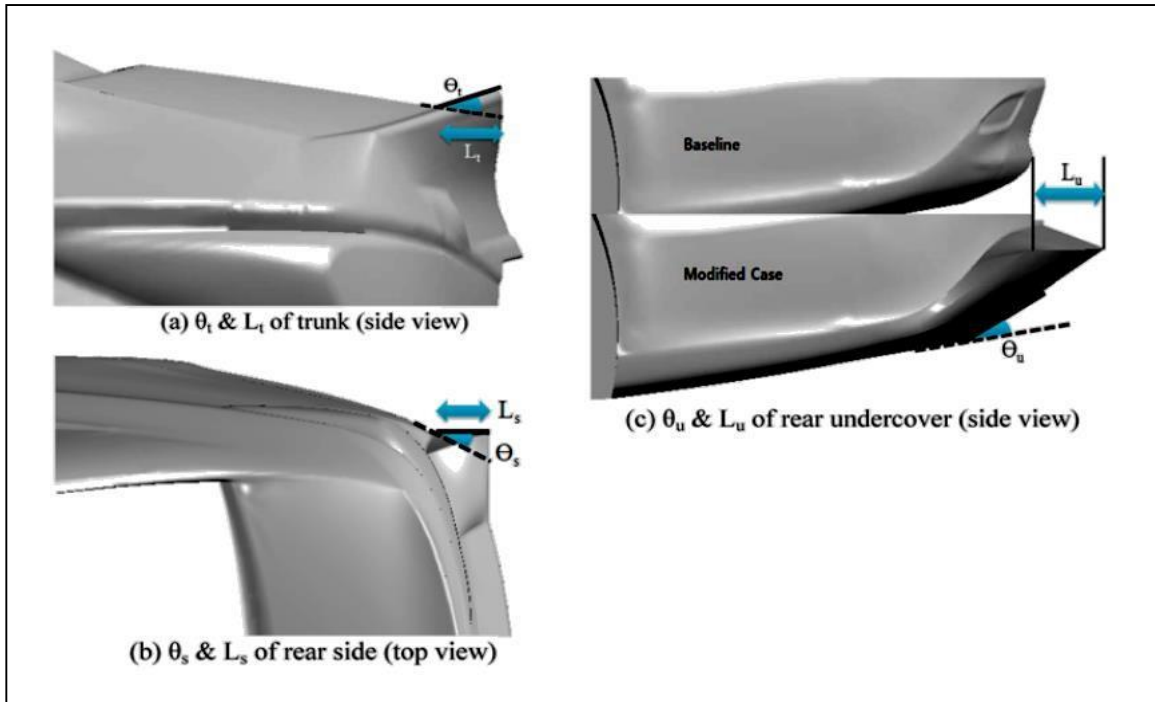


Figure 2.3(xvi): Concept of design variables [55]

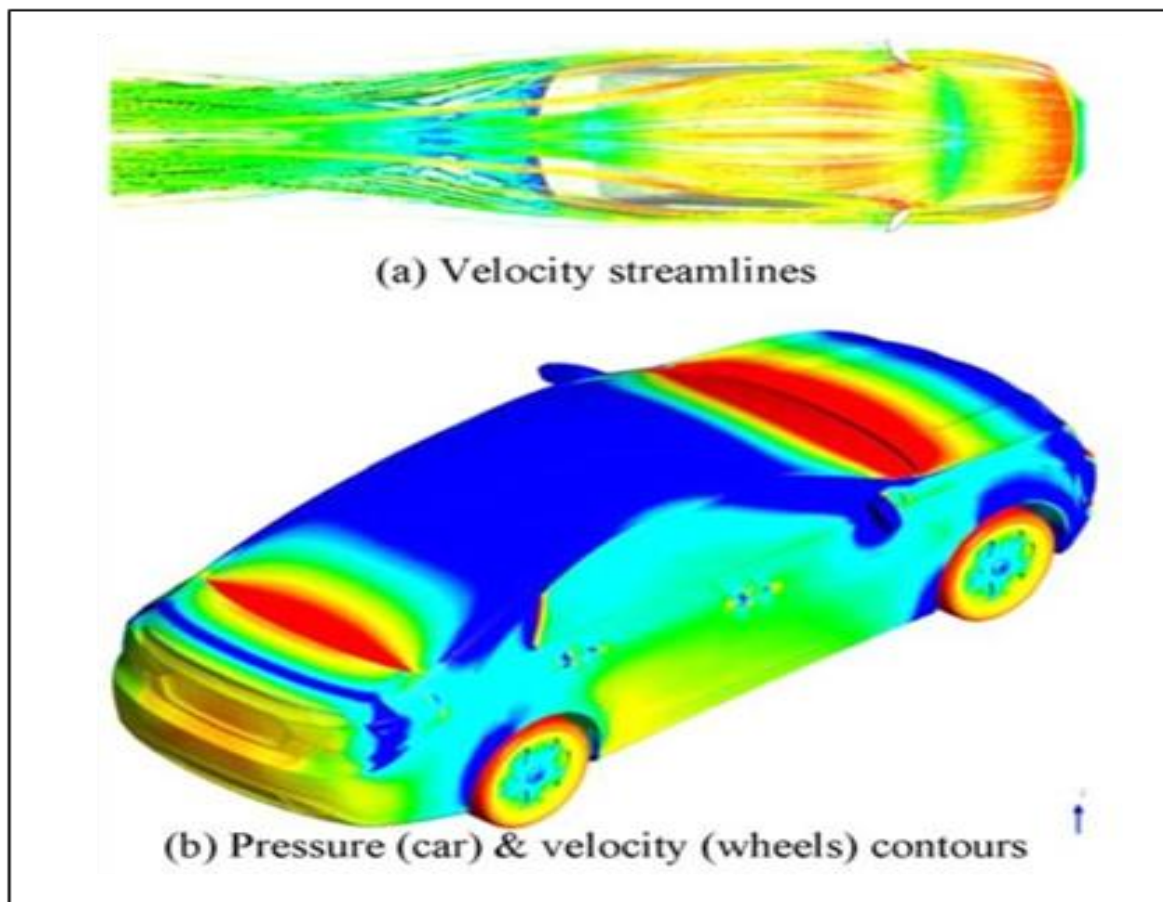


Figure 2.3(xvii): Example of CFD simulation result [55]

3. METHODOLOGY

3.1 ANSYS:

ANSYS is software used in finite element analysis package (FAE) code for the computer-aided engineering (CAE) field. ANSYS software is used for the construction of computer models solving various mechanical problems such as structures, machine components or systems with applying and operating loads and other design criteria of the study of physical responses including stress levels, structural analysis, heat transfer, temperature distributions fluid problems, pressure etc.

The software is used by following basic procedure:

- 1. Pre-processing:** In the pre-processing method, a geometry (physical bounds) of the problem is defined. The volume engaged by the fluid has been divided into a no. of discrete cells which is called mesh. This mesh can be either uniform or non-uniform. The physical modelling is interpreted, for example, the equations of motion + enthalpy + radiation + species conversion Boundary conditions are interpreted. This included particulate the fluid behaviour of the problem but as for the transient problems, concluded boundary conditions are also designated.
- 2. Solving:** The coding computational methods are done here and solving process is required. The simulation is started and the equations are solved iteratively consideration physical phenomena.
- 3. Post- processor:** Here, the results obtained are visualized and analyzed by this process which can verify the results and if possible, conclusions can be brought affirmatively based on the result.

3.2 ANSYS & CAD Theory

3.2.1 CAD design

To achieve the results in the analysis of the aerodynamics, we have to work in one CAD program to simulate the geometry of the car and the roof box and the program is used in Solid Works. It has two ways to simulate and these are - (i) create a 2 dimensional profile

with a surface and export it to Ansys Fluent, (ii) create the design in 3 dimensions model and also export to Ansys Fluent..

To create the most similar original model feasible, we first have the information on the sizes and surfaces of the bodies. The little surfaces on the top of the roof box were disregarded because their purpose was aesthetics rather than aerodynamics.

3.2.2 Modelling

We import the geometry into Ansys Fluent after it has been produced. As a result, the solution suggests saving the geometry as a file in a neutral format (IGES, STEP...). After that, using the geometry we have been given, we can complete this project's job. The geometry produced depicts the wind tunnel air flow. The goal is to study in a worthless, empty area. The body's components are renamed in this section as well.

It is different from studying aerodynamics in two dimensions to study aerodynamics in three dimensions. To import our geometry, we must first design it in both 2 and 3 dimensions. We just need to research half of the assembly because of its symmetry. Then, using the sketch, we draw a box to represent the surrounding air around the geometry. The following step involves using the Boolean condition to subtract the original geometry and produce a box with an empty assemblage inside of it.

3.2.3 Meshing

Mesh creation comes next after modelling technique. It is one of the crucial phases in using FEA to perform the appropriate simulation. A mesh is consisted up to parts that contain nodes having coordinate locations in space that can vary by element type that represent the shape of the geometry. An FEA solver cannot easily work with irregular shapes, but it is abundant happier with common shapes like cubes. Meshing is the the method of turning irregular shapes into additional recognizable volumes known as “elements”. These feature makes it very straightforward to compute using numerical methods and obtain accurate data. The questionnaires to gather parameters were used to generate a large density grid, and as a response, the best possible outcomes were obtained:

- **Elements:** The selection of the most appropriate component is the most crucial step in the meshing process. We prefer to choose quadrilateral parts, which give an accurate

outcome of the aerodynamic, in order to get a simple outcome. However, there are a few problems that prohibit anyone from using a high-density mesh in the three-dimensional analysis, therefore we should switch towards another method.

- **Sizing:** within the initial analysis we have a tendency to use a mesh with larger values of parts to get to obtain a reference of the results and verify if the method used is that the correct. To obtain the proper results, we changed these values. Modifying these values, we have a tendency to get a high-density mesh and therefore the result is additionally correct..
- **Inflation:** The decision of the turbulence model and, subsequently, the flow field we have a propensity to be concerned in will influence either we determine the entire profile of the physical phenomena as boundary or, as a backup plan, if we use realistic facilities in order to reduce the cell count. If we look at the images below, we will notice that the physical phenomenon profile is simulated with a diminished cell on the left facet, which really is typical of a wall operational technique. The physical phenomenon pattern is completed all the way to the barrier on the right, adjusted for inflation. This might provide a further precise understanding for the scientific principle.

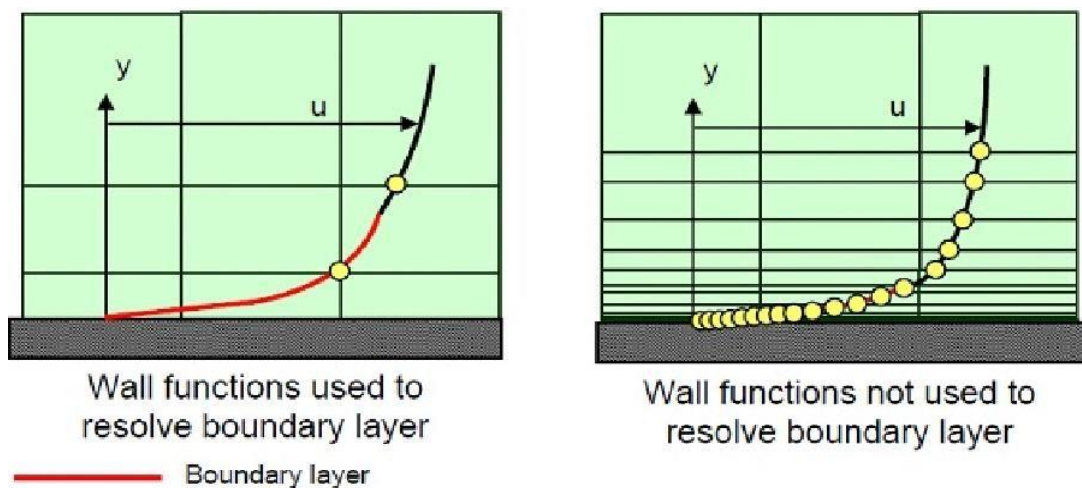


Figure 3.2.3: Inflation in boundary layer

3.2.3.1 TYPES OF MESHING MODELS:

There are typically two types of meshing methods. For these purposes, we are referring to 3D models:

- Tetrahedral element meshing or “tet”

- Hexahedral element meshing or “hex”

Hex or “brick” parts typically lead to additional correct results at lower element component counts than tet elements. If it is a complex geometry, tet elements is the simplest alternative. These default or automatic meshing strategies is also enough to induced you whenever you need to go, however, there are additional strategies that can provided you with additional of mesh management. Simply put, a good quality mesh equals more precise results. A poor mesh can result in convergence difficulties, which may result in incorrect results and false conclusions.

Meshing controls modify additional precise mesh. Ansys Mechanical allowss you to regulated local meshes rather than a global mesh that meshes the whole CAD with the equivalent methods. Some examples of native meshing controls embody native filler, refinement and sphere of influence defeaturing of the pure geometry.

3.2.4 Analysis

The three primary factors—fluid, fluid speed, and impact area—have been taken into account in the analysis of the entire car body, which uses a model to discover the values.

- ***K-EPSILON(ϵ) turbulence model***[64]:

This model simulates turbulent conditions in computational fluid dynamics (CFD). It is primarily based on two equations that, using two transport equations, give an outline of turbulence.

The K-epsilon model was first developed to improve the mixing-length model and provide an alternative to algebraically defining turbulent length scales in flows with moderate to high complexity. The principal conveyed variable, also known as turbulent kinetic energy, may control the energy contained in the turbulence (k). The turbulent dissipation, which controls how quickly the turbulent kinetic energy dissipates, is the second transferred variable.

For turbulent kinetic energy k

$$\frac{\partial}{\partial t}(\rho\epsilon) + \frac{\partial}{\partial x_i}(\rho\epsilon u_i) = \frac{\partial}{\partial x_j} \left[\left(\mu + \frac{\mu_t}{\sigma_\epsilon} \right) \frac{\partial \epsilon}{\partial x_j} \right] + C_{1\epsilon} \frac{\epsilon}{k} (P_k + C_{3\epsilon} P_b) - C_{2\epsilon} \rho \frac{\epsilon^2}{k} + S_\epsilon$$

For dissipation ϵ

$$\frac{\partial}{\partial t}(\rho\epsilon) + \frac{\partial}{\partial x_i}(\rho\epsilon u_i) = \frac{\partial}{\partial x_j} \left[\left(\mu + \frac{\mu_t}{\sigma_\epsilon} \right) \frac{\partial \epsilon}{\partial x_j} \right] + C_{1\epsilon} \frac{\epsilon}{k} (P_k + C_{3\epsilon} P_b) - C_{2\epsilon} \rho \frac{\epsilon^2}{k} + S_\epsilon$$

u_i : velocity component in corresponding direction

E_{ij} : component of rate of deformation

μ_t : eddy viscosity

- **Fluid-Air:**

It is important to specify the fluid in Ansys' input values. It should be noted that the fluid is air and that its density is controlled by its temperature. The most common and widespread one is temperature gain. Here, 288.16K was used, and air has a density of 1.225 kg/m³.

- **Velocity:**

When simulating automobile-related events, we frequently assume that the vehicle is moving at 72 km/h (20 m/s) while not in a transverse wind (the air only appears on direction x). As a result, once these values must be entered into Ansys, we must assume that the car is stopped and that the only thing moving is the air.

- **Frontal Area:**

Considering the many scenarios where the value of the front area changes, we must in this instance place the projected region that affects the car, which is clearly visible from the front.

3.2.5 Results obtained through above method

After running the calculation the values that actually interest in our study to analyse area of the coefficient of drag, pressure, velocity, turbulence and Reynolds. To get these values, the program runs iterations to find the convergence solution. In some cases the convergence is not possible and therefore the decision that is taken is running with addition of calculations to find a stabilized solution. In this way we may have got values of our results with a low oscillation. Depending on the case (if it is 2 dimensional or 3 dimensional) the solution is stabilized quicker or slower. In analysis of two dimension with having less than 100 iterations, we are able to acquire a converged solution. On the other hand, for 3 dimensional analysis, it's required nearly at least 500 iterations to get a stable solution. One of the main results required to the presents of this project is coefficient of drag and therefore, the drag

force generated because of the change of speed and the different dimension changes. The pressure permits knowing wherever the elements are affected by fluid with more high pressure of air and where the dynamic pressure amounts zero. This distinction of pressure is useful as well to know which air resistance should beat the car. The velocity plots are helpful to know what is the purpose of the point of effect of the car is, since the speed in this point is 0 m/s. With this plot, we are also able to compare simultaneously the speed between the top and the beneath of the car and where the biggest speed is located. Finally, the turbulence and Reynolds plots permits the analyse how the fluid is concerned and reckoning on the shapes of the cars. The turbulence shows the range where the fluid can have less momentum diffusion, large momentum convection and speedy changes of pressure and velocity in space and time.

4. RESULTS AND DISCUSSIONS

4.1 CASE I- Comparison of cuboidal truck having sharp edges and cuboidal truck having circular edges:

For comparing the drag force and the drag coefficients of both these models I first chosen a cuboidal structure which seems like a truck and by doing analysis using Ansys software I got results as follows.

Dimension of the cuboidal truck,

Length (l):2.5m, width (w):0.32m and height (h):0.46m

Dimension of the wind tunnel (encloser),

Length (L):16m, width (W):3m and height (H):2.2m

In all cases I have taken same conditions in ansys software as:

- Time – Steady
- Viscous – Standard K-epsilon turbulence model
- Wall treatment – Standard wall function
- Turbulent specification method – Intensity & Hydraulic Diameter
- Turbulent intensity (at inlet) – 5%
- Turbulent intensity (at outlet) – 5%

For making the edges rounder I provided fillet radius equals to 0.2m in every corner of the above dimension. After providing these geometries in the ansys software and performing simulation I got these in both these cases.

In figure 4.1(i) and figure 4.1(ii), geometry of cuboidal truck having sharp edges and circular edges are compared. It can be observed from the provided geometry that there are changes regarding curvature of the edges. As per this geometrical criterion, further results are obtained.

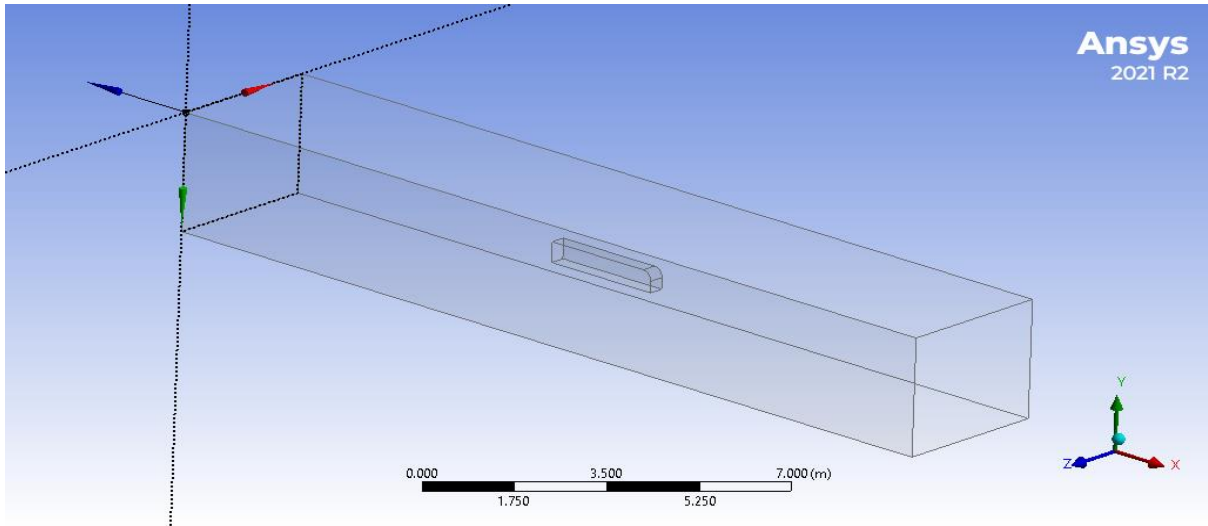


Figure 4.1(i):- Geometry used in ansys of cuboidal truck having sharp edges

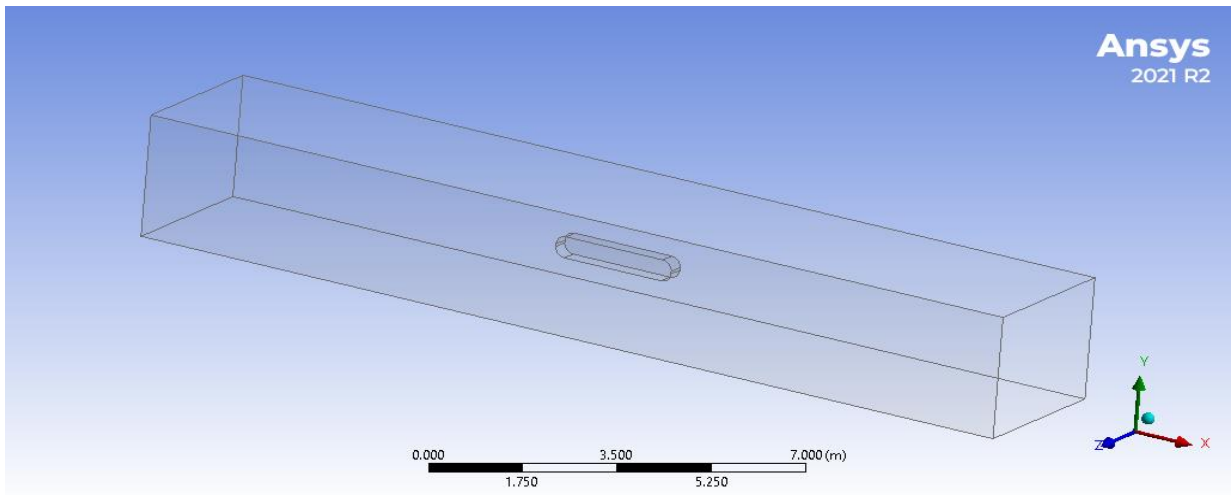


Figure 4.1(ii):- Geometry used in ansys of cuboidal truck having circular edges

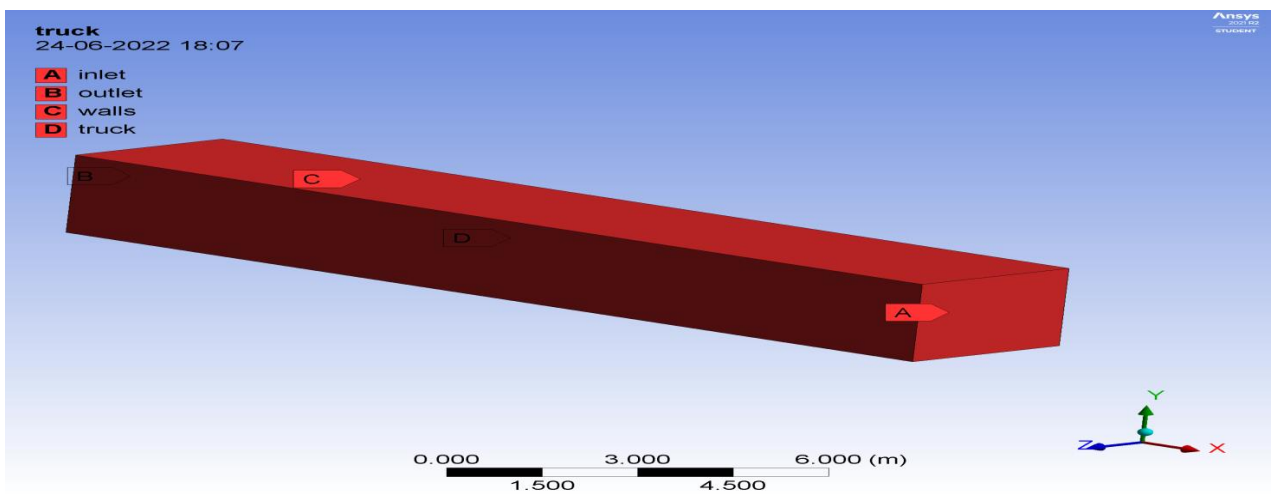


Figure 4.1(iii):- Named selection for both cases

The following figure (Figure 4.1(iii)) shows the named selection for the model. Where inlet, outlet, walls of body and overall body surfaces are specified.

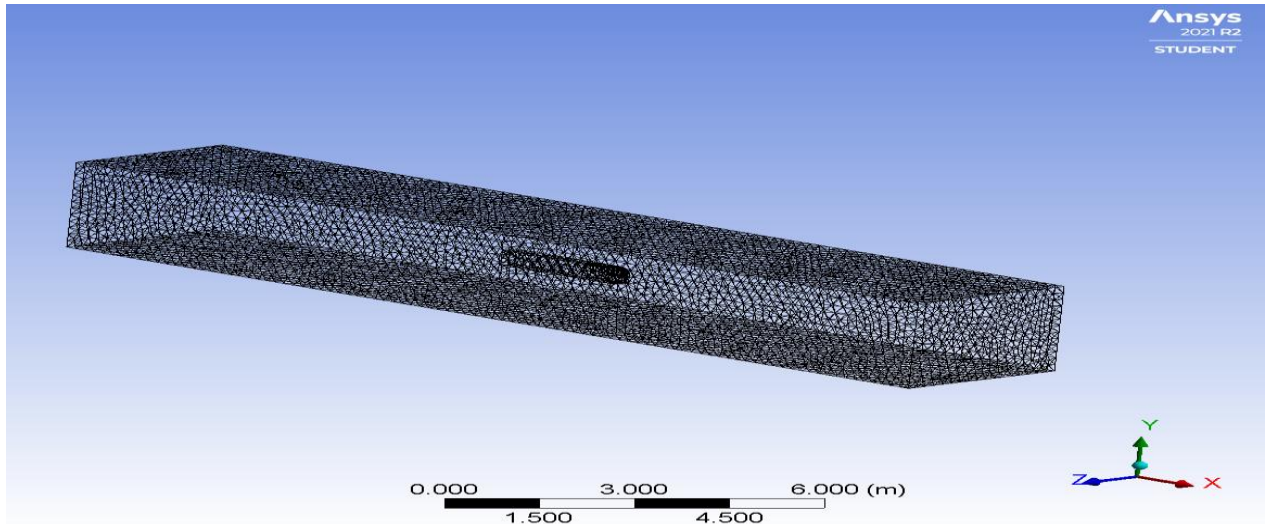


Figure 4.1(iv):-mesh of sharp edge truck

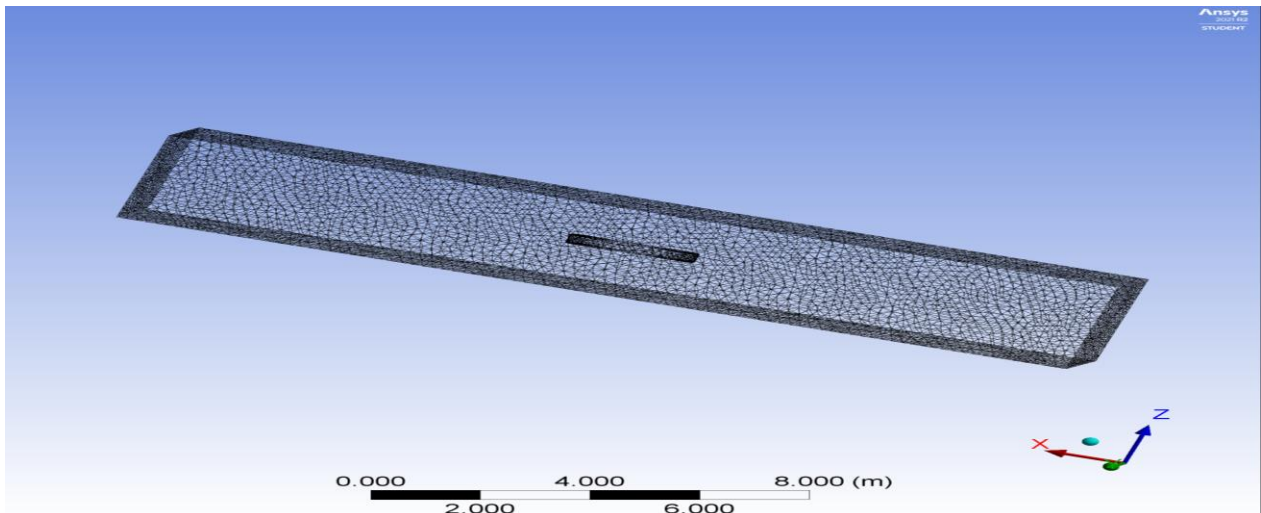


Figure 4.1(v):-mesh of circular edge truck

Figure 4.1(iv) shows the mesh generated for the designed sharp edged body where hexahedral meshing is done with number of cells = 33326, number of faces = 182492, and number of nodes = 137272.

Figure 4.1(v) shows the mesh generated for the designed circular edged body where hexahedral meshing is done with number of cells = 32104, number of faces = 188998, and number of nodes = 148672.

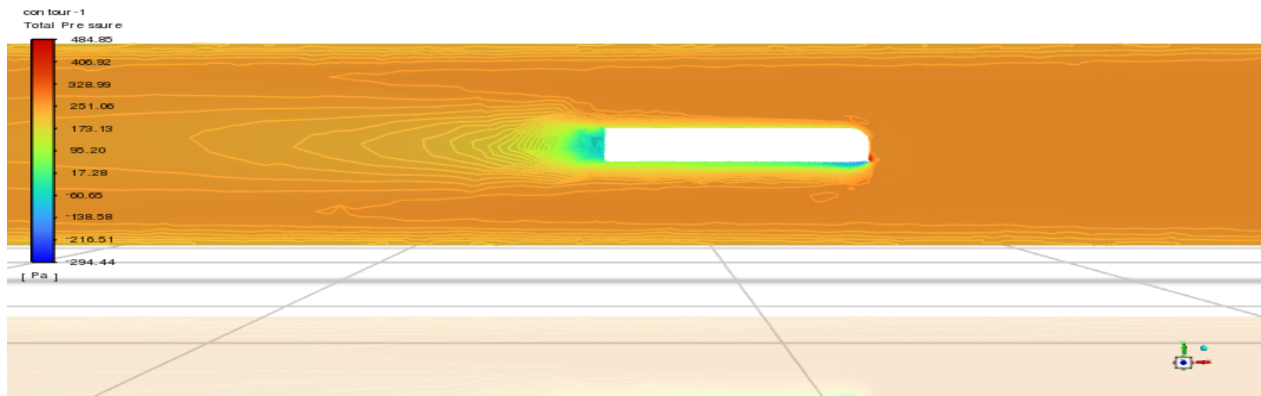


Figure 4.1(vi):- total pressure contour for sharp edge

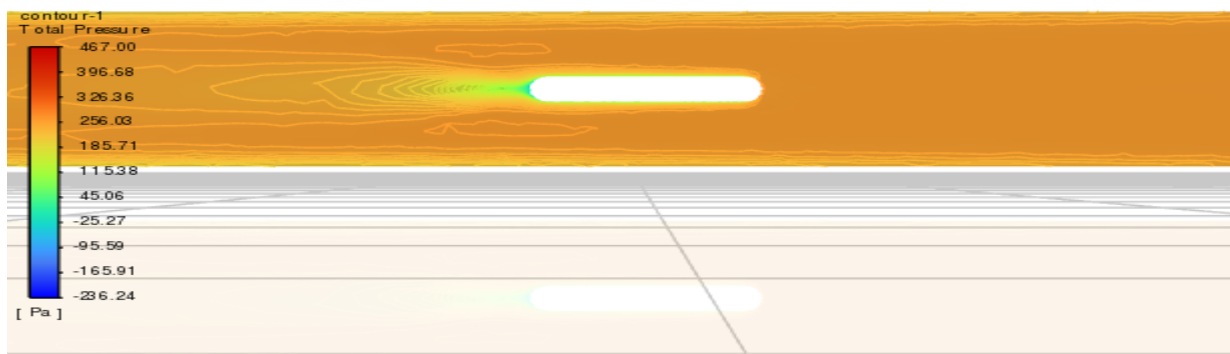


Figure 4.1(vii):- total pressure contour for circular edge

The above Figure 4.1(vi) shows the total pressure contour for sharp edges where minimum obtained total pressure is 204.44 (pa) and maximum pressure obtained is 484.80 (pa).

The above Figure 4.1(vii) shows the total pressure contour for circular edges where minimum obtained total pressure is -296.24 (pa) and maximum pressure obtained is 467.00 (pa).

It can be seen that greater wake region is obtained on the back side (can be seen on left side of the body) of the body in downstream. Whereas wake region obtained for the circular edged body is lower than the former one.

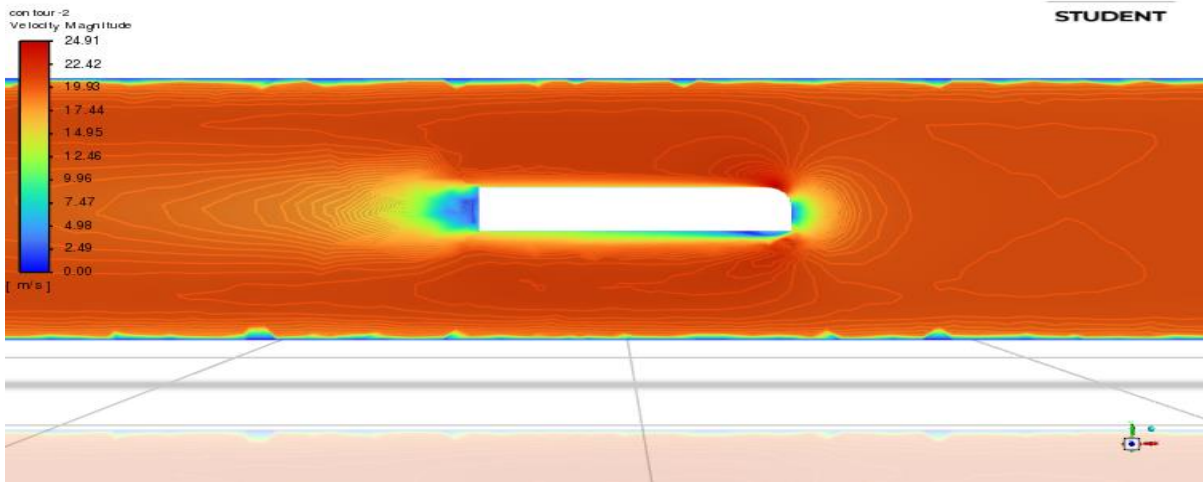


Figure 4.1(viii):-velocity contour for sharp edge

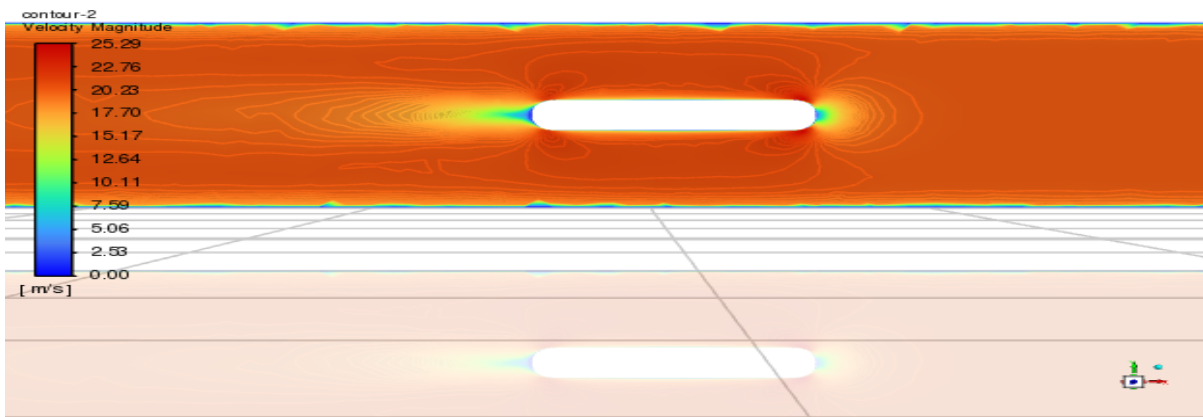


Figure 4.1(ix):-velocity contour for circular edge

In the above Figure 4.1(viii), velocity contour for sharp edged body is shown, where the velocity magnitude ranges from 0-24.91 m/s.

In the above Figure 4.1(ix), velocity contour for circular edged body is shown, where the velocity magnitude ranges from 0-25.29 m/s, Which is higher velocity than former case.

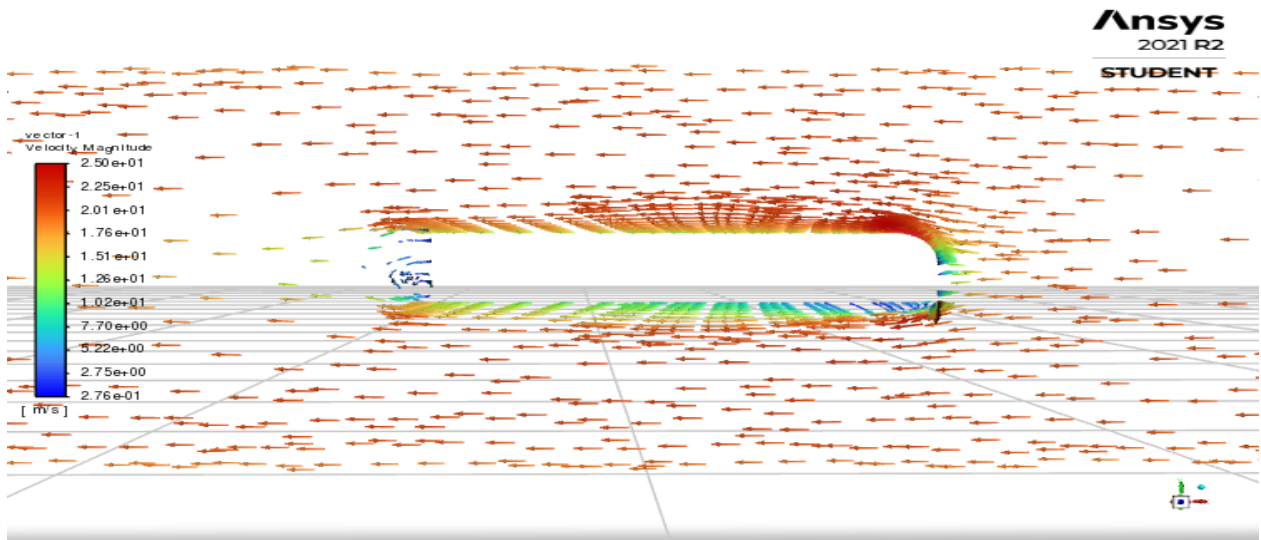


Figure 4.1(x):-velocity vector for sharp edge

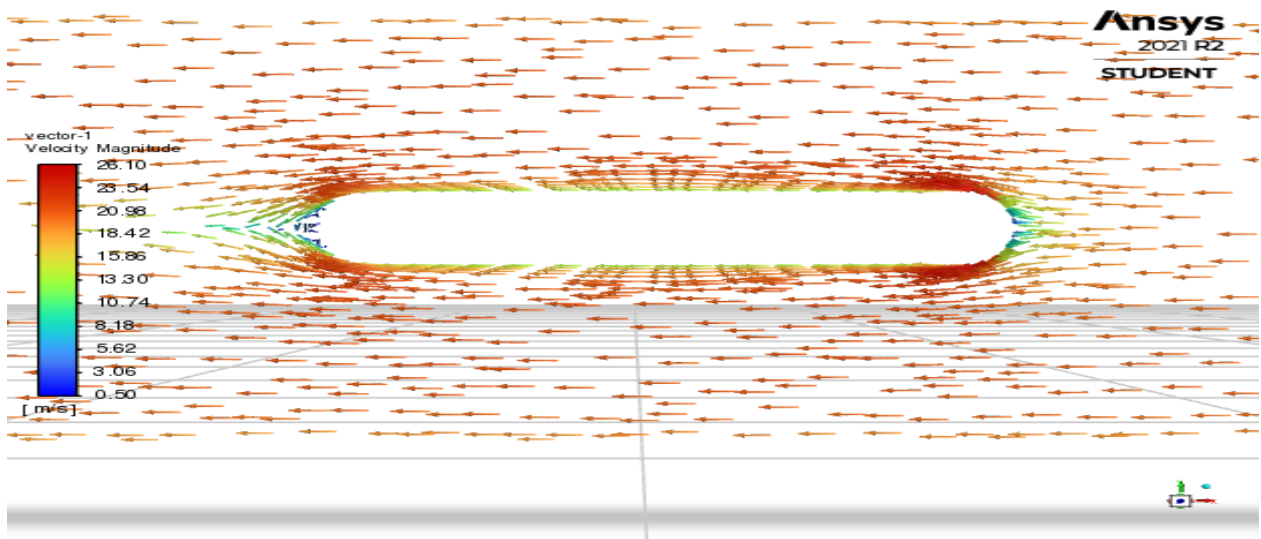


Figure 4.1(xi):-velocity vector for circular edge

Cuboidal truck having sharp edges-

During meshing , element size = 0.2m, Nodes = 23695, Elements = 113087.

Dimension of the cuboidal truck,

Length (l):2.5m, width (w):0.32m and height (h):0.46m

Dimension of the wind tunnel (encloser),

Length (L):16m, width (W):3m and height (H):2.2m

$$\text{Projected area (A}_P\text{)} = 0.1472 \text{ m}^2$$

During simulation I performed 800 iterations in which it get fully converged around 319 iterations and in this I get,

$$\begin{aligned}\text{Hydraulic Diameter (D}_H\text{)} &= 4 \cdot A/P \\ &= \mathbf{2.954m}\end{aligned}$$

Using this and considering the velocity of vehicle 20m/s(=72km/h) I got the drag coefficient(C_D) value = **1.0778** and the drag force(F_D) value = **38.872N**

Cuboidal truck having circular edges-

During meshing, element size = 0.2m, Nodes = 25997, Elements = 126418.

Dimension of the cuboidal truck,

$$\text{Length (l):2.5m, width (w):0.32m and height (h):0.46m;}$$

Dimension of the wind tunnel (encloser),

$$\text{Length (L):16m, width (W):3m and height (H):2.2m;}$$

$$\text{Projected area(A}_P\text{)} = 0.1472 \text{ m}^2$$

During simulation I performed 1600 iterations in which it get partially converged and in this I get,

$$\begin{aligned}\text{Hydraulic Diameter(D}_H\text{)} &= 4 \cdot A/P \\ &= \mathbf{2.954m}\end{aligned}$$

Using this and considering the velocity of vehicle 20m/s(=72km/h) I got the drag coefficient(C_D) value = **0.652** and the drag force(F_D) value = **23.5172N**.

4.2 CASE II- Comparison between Ahmed body having closed windows and Ahmed body with open windows:-

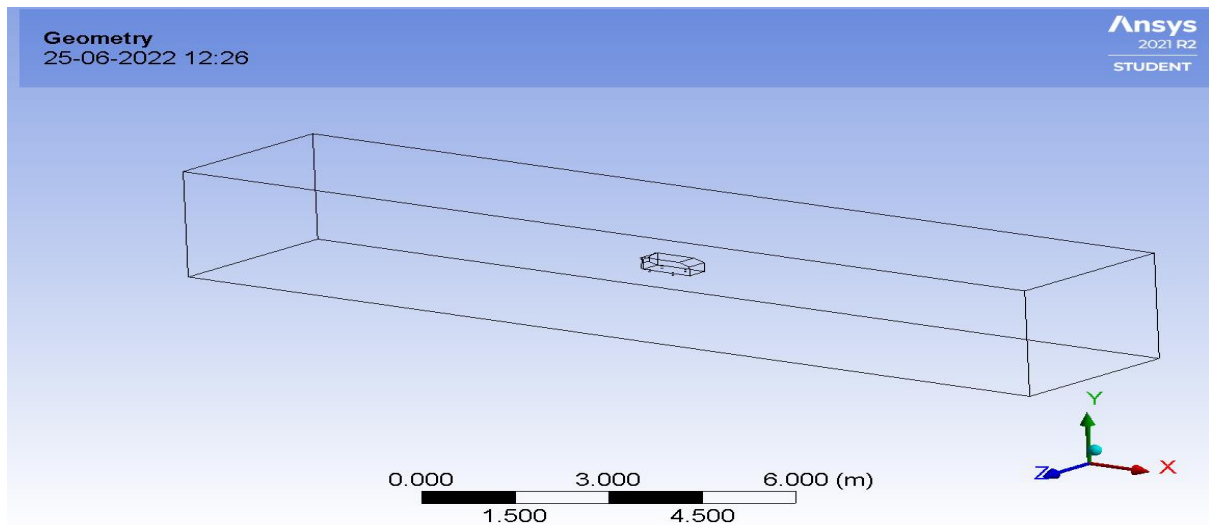


Figure 4.2(i):-Geometry of Ahmed body

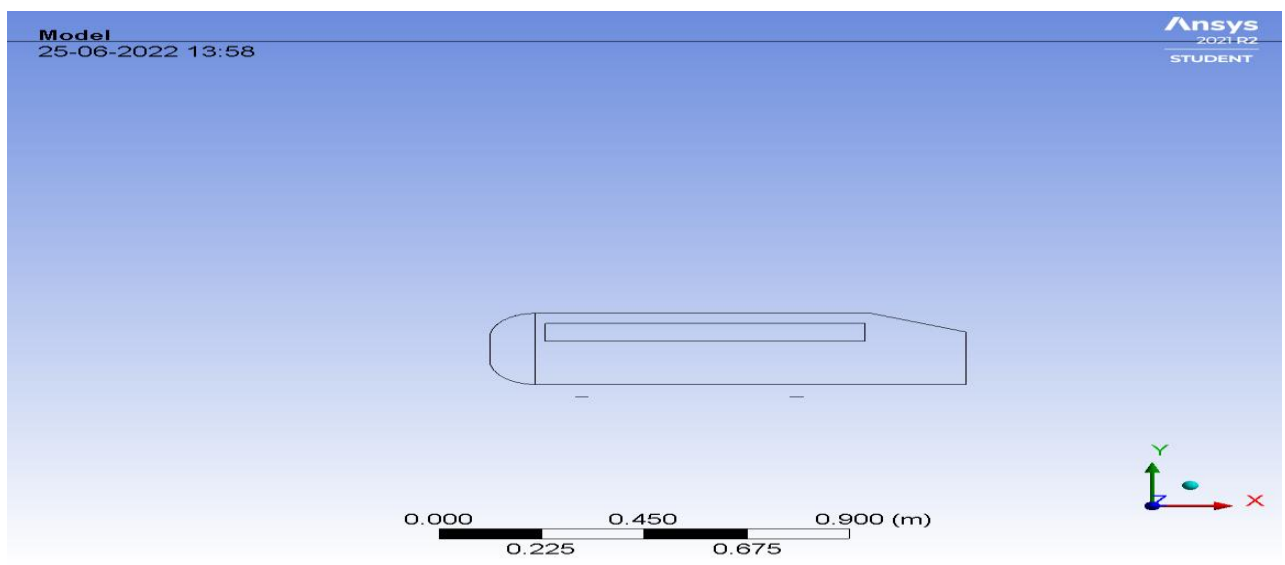


Figure 4.2(b):- Geometry of Ahmed body with open windows

In above figures Figure 4.2(i) and Figure 4.2(ii), geometry of Ahmed body with closed windows and Ahmed body with open windows are compared. It can be observed from the provided geometry that there are aerodynamic conditions are changed. As per this geometrical criterion, further aerodynamic parameters are obtained.

The following figure (Figure 4.2(iii)) shows the named selection for the model. Where inlet, outlet , enclosure walls and the body surfaces of car is specified.

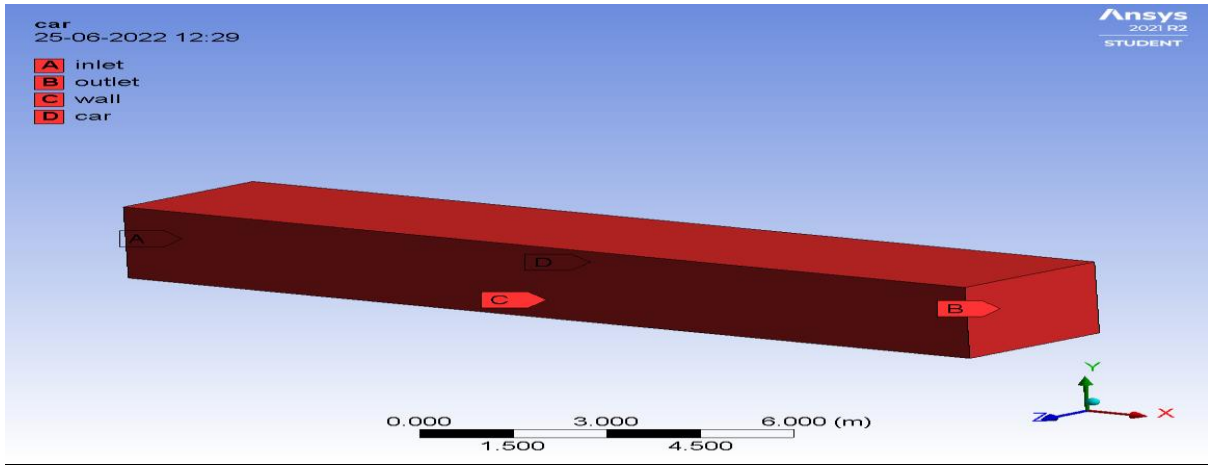


Figure 4.2(iii):-Named selection for both the cases

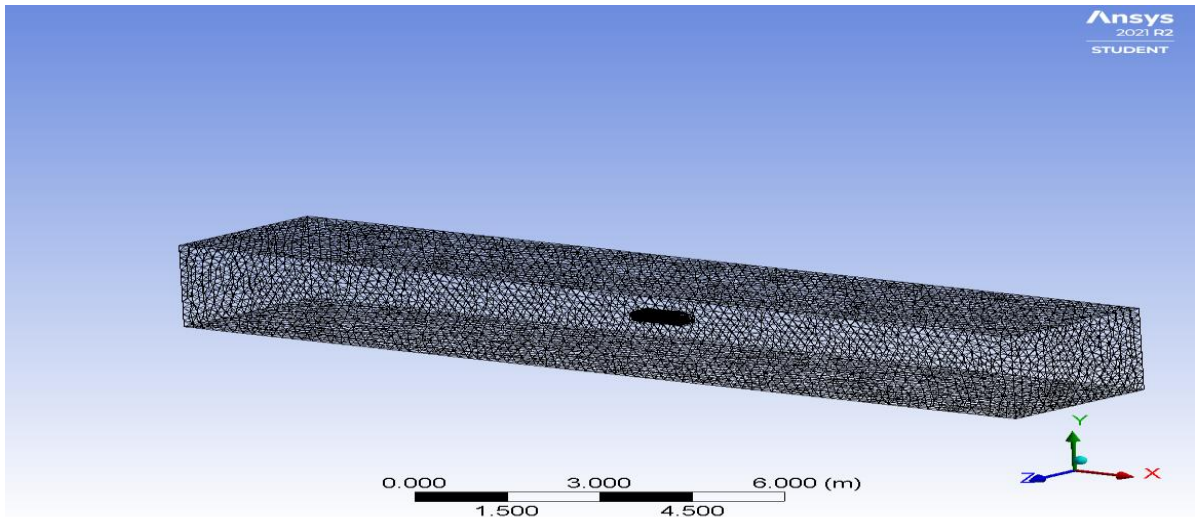


Figure 4.2(iv):- Mesh for Ahmed body

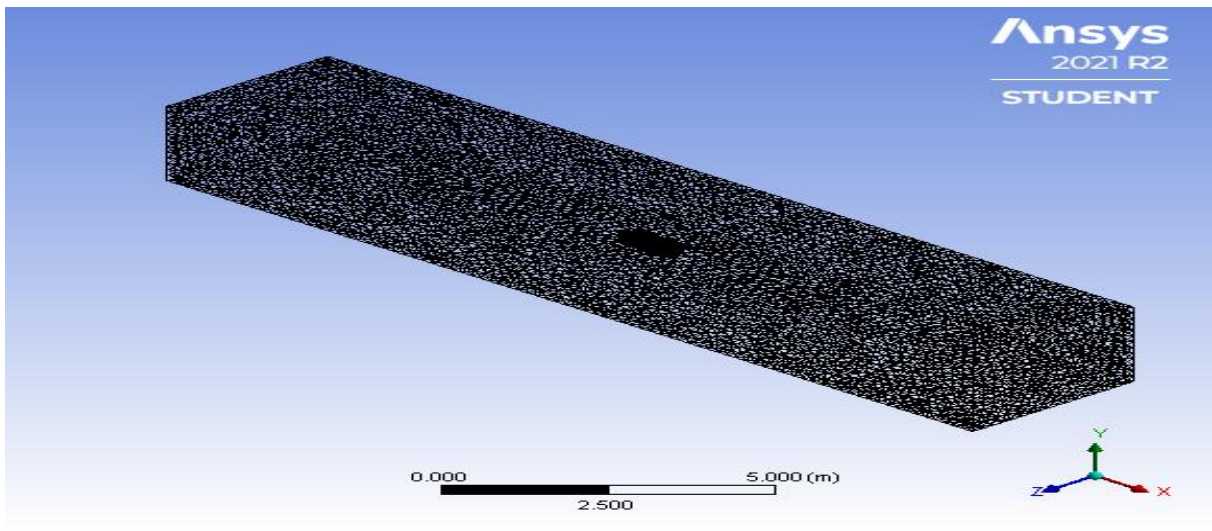


Figure 4.2(v):- Mesh for Ahmed body with open windows

Figure 4.2(iv) shows the mesh generated for the designed Ahmed body with closed windows is shown, where hexahedral meshing is done with number of cells = 71296 , number of faces = 380261, and number of nodes = 276564.

Figure 4.2(v) shows the mesh generated for the designed Ahmed body with open windows is shown, where hexahedral meshing is done with number of cells = 79474, number of faces = 407854, and number of nodes = 287970.

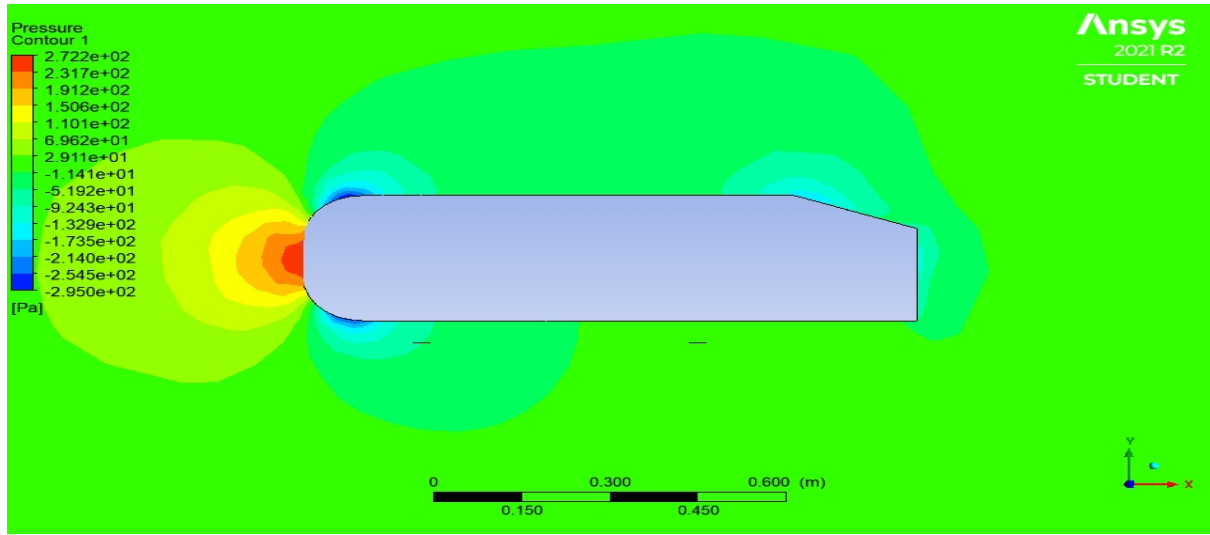


Figure 4.2(vi):- Pressure contour for Ahmed body

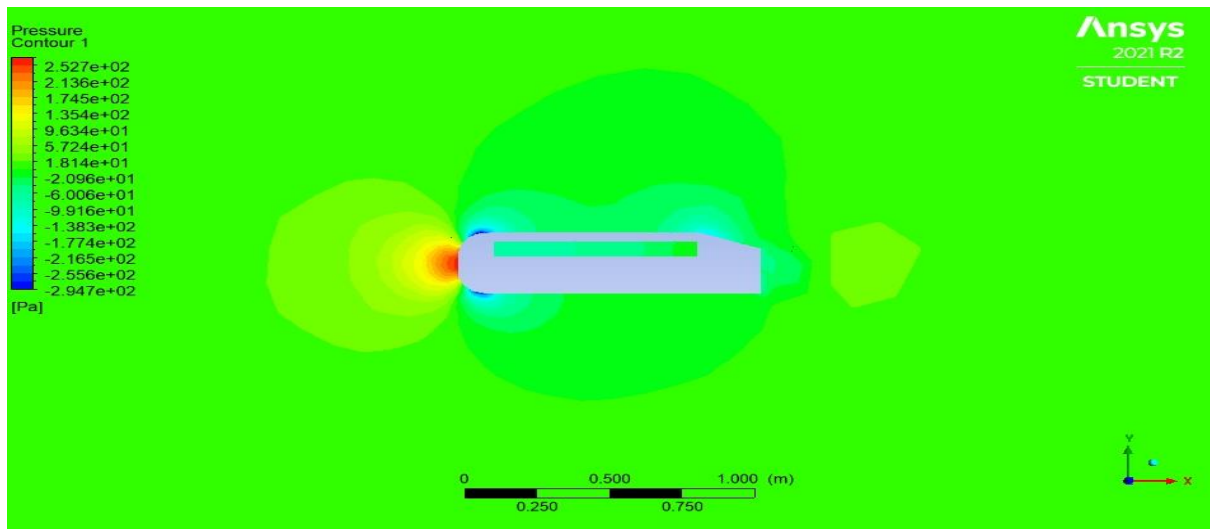


Figure 4.2(vii):- Pressure contour for Ahmed body with open windows

The above Figure 4.2(vi) shows the total pressure contour for Ahmed body with closed windows is shown where minimum obtained total pressure is -295.0 (pa) and maximum pressure obtained is 272.2 (pa).

The above Figure 4.2(vii) shows the total pressure contour for Ahmed body with open windows is shown where minimum obtained total pressure is -294.7 (pa) and maximum pressure obtained is 252.7 (pa).

It can be seen that there is similar maximum and minimum pressure variation is observed for both the cases. Here we can observe from the above contours that the similar wake region can be obtained for both the cases.

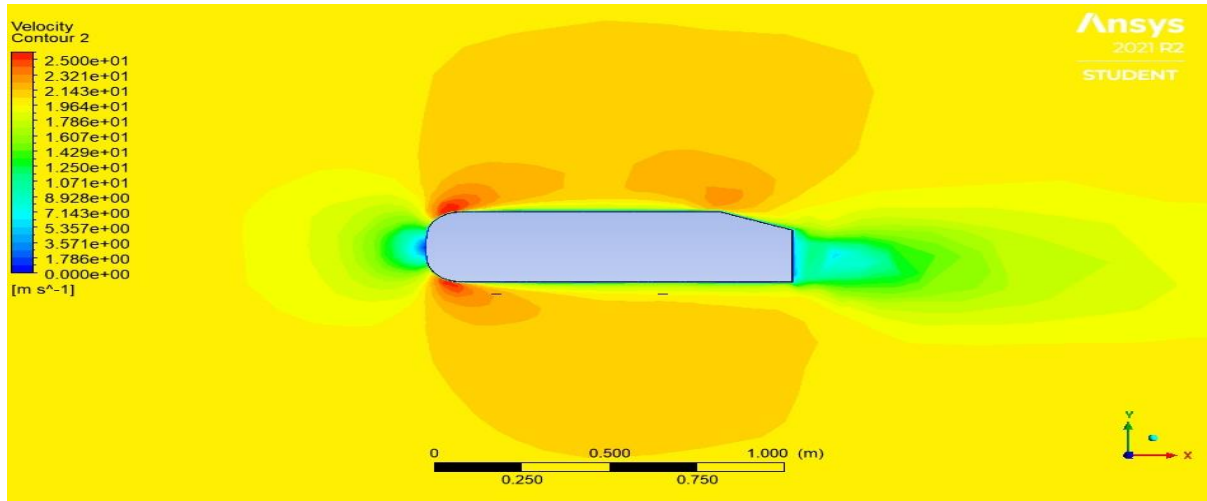


Figure 4.2(viii):- Velocity contour for Ahmed body

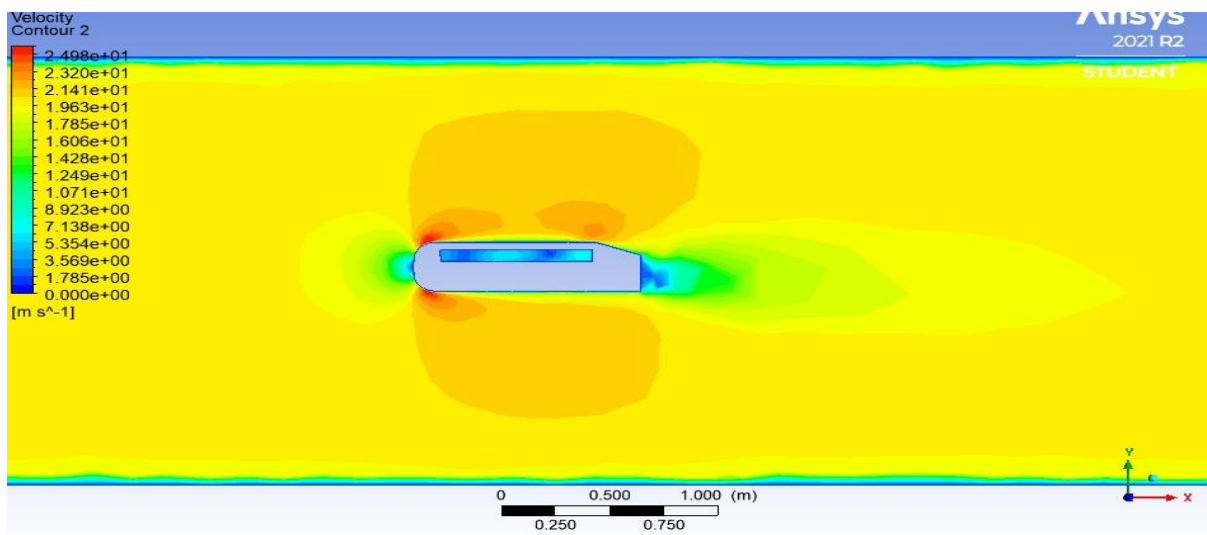


Figure 4.2(ix):- Velocity contour for Ahmed body with open windows

In the above Figure 4.2(viii), velocity contour for Ahmed body with closed windows is shown, where the velocity magnitude ranges from 0-25.0 m/s.

In the above Figure 4.2(ix), velocity contour for Ahmed body with open windows is shown, where the velocity magnitude ranges from 0-24.98 m/s, which is similar velocity than former case.

Here for the Ahmed body with open windows, turbulence generation is observed , resulting in an increment in drag force.

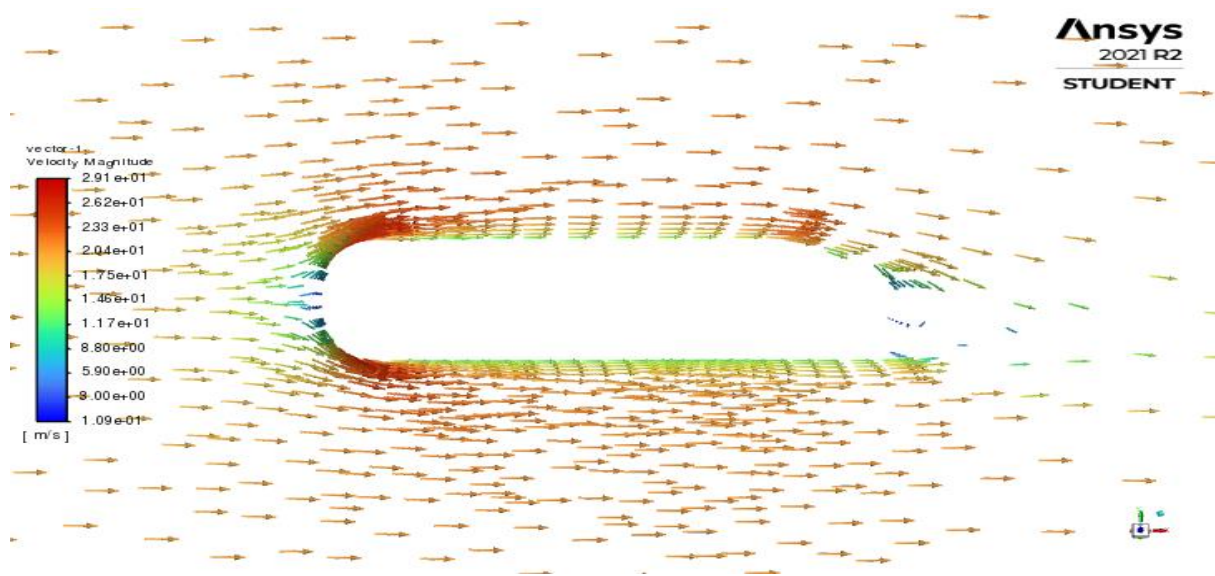


Figure 4.2(x):- Velocity vector for Ahmed body

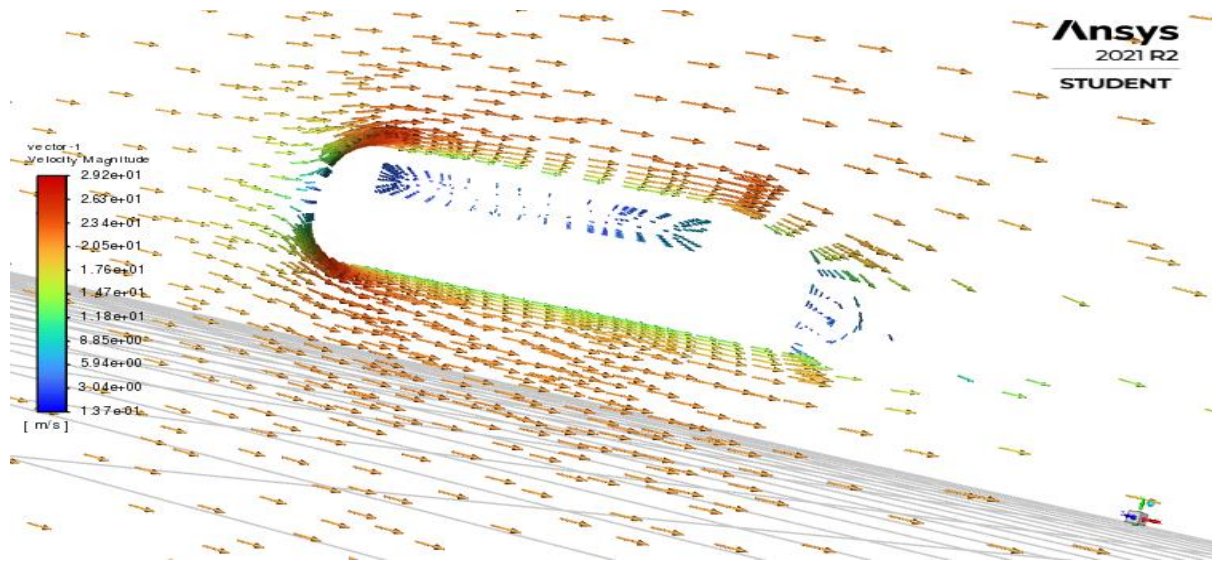


Figure 4.2(xi):- Velocity vector for Ahmed body with open windows

Ahmed body having closed windows-

During meshing, element size = 0.2m, Nodes = 276564, Cells = 71296, Faces = 380261.

$$\text{Projected area}(A_P) = 0.1150138 \text{ m}^2$$

Enclosure, L= 16m, W=3m, H=2.2m.

$$\begin{aligned}\text{Hydraulic Diameter}(D_H) &= 4 \cdot A/P \\ &= 2.87\text{m}\end{aligned}$$

During simulation, I performed 1000 iterations in which it partially converged and in this I get,

Using this and considering the velocity of vehicle 20m/s(=72km/h) I got the drag coefficient(C_D) value = **0.55** and the drag force(F_D) value = **15.5N**

Ahmed body with open windows -

During meshing , element size = 0.2m, Nodes = 287970, Cells = 79474, Faces = 407854.

$$\text{Projected area}(A_P) = 0.1150138 \text{ m}^2$$

$$\text{Window size} = 0.7 \cdot 0.07 \text{ m}^2$$

Enclosure, L= 16m, W=3m, H=2.2m.

$$\begin{aligned}\text{Hydraulic Diameter}(D_H) &= 4 \cdot A/P \\ &= 2.87\text{m}\end{aligned}$$

During simulation I performed 1600 iterations in which it get partially converged and in this I got,

Using this and considering the velocity of vehicle 20m/s(=72km/h) I got the drag coefficient(C_D) = **0.5911** and the drag force(F_D) = **16.656N**.

% change increase in drag coefficient = **7.5%**

4.3 CASE III- Comparison between Ahmed body and Ahmed body with blower at the top:-

In following figures Figure 4.3(i) and Figure 4.3(ii), geometry of Ahmed body and Ahmed body with blower attached to the top are compared. It can be observed from the provided modifications the aerodynamic conditions, the drag coefficients, drag forces are changed. As per this geometrical criterion, further aerodynamic parameters are compared.

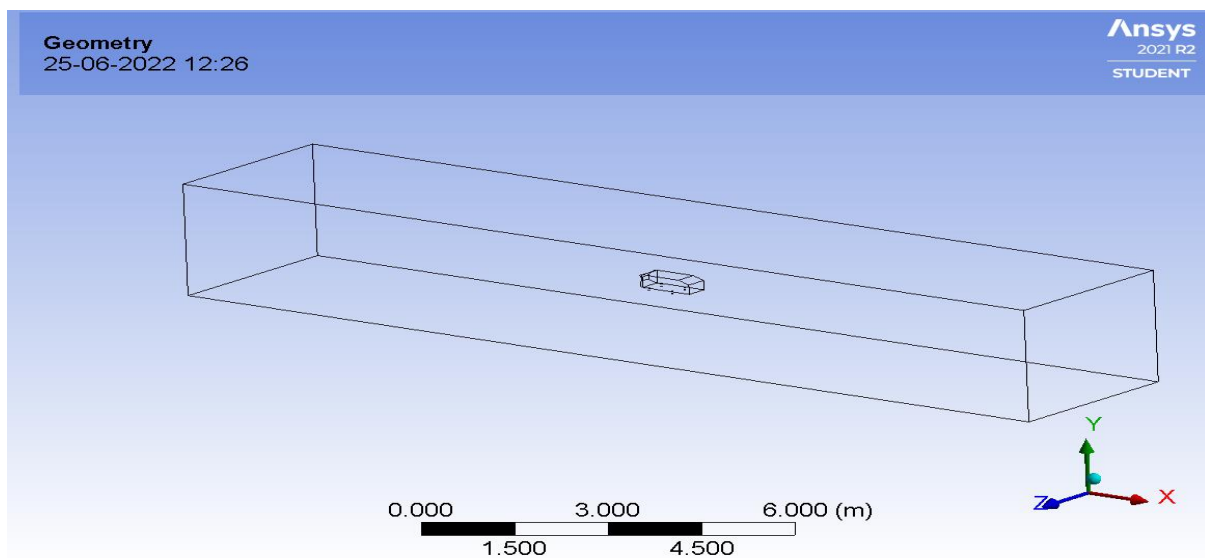


Figure 4.3(i):-Geometry of Ahmed body

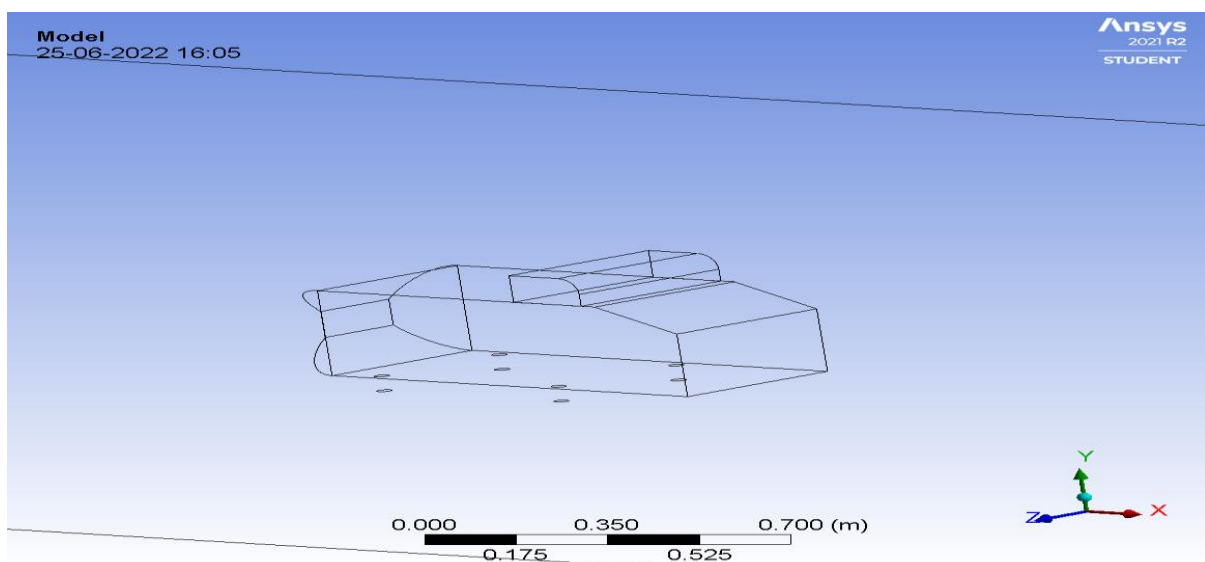


Figure 4.3(ii):-Geometry of Ahmed body with blower at its top

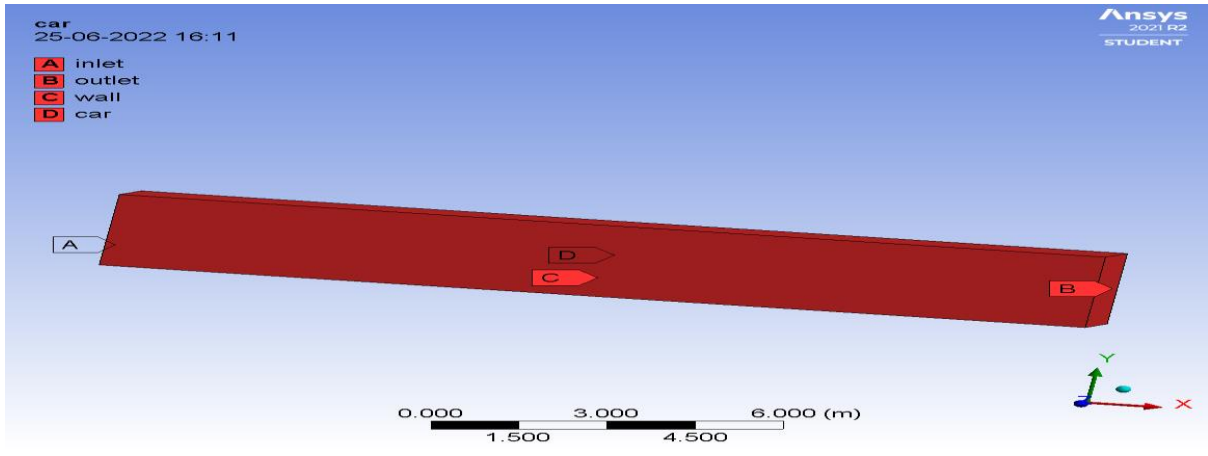


Figure 4.3(iii):-Named selection for both the cases

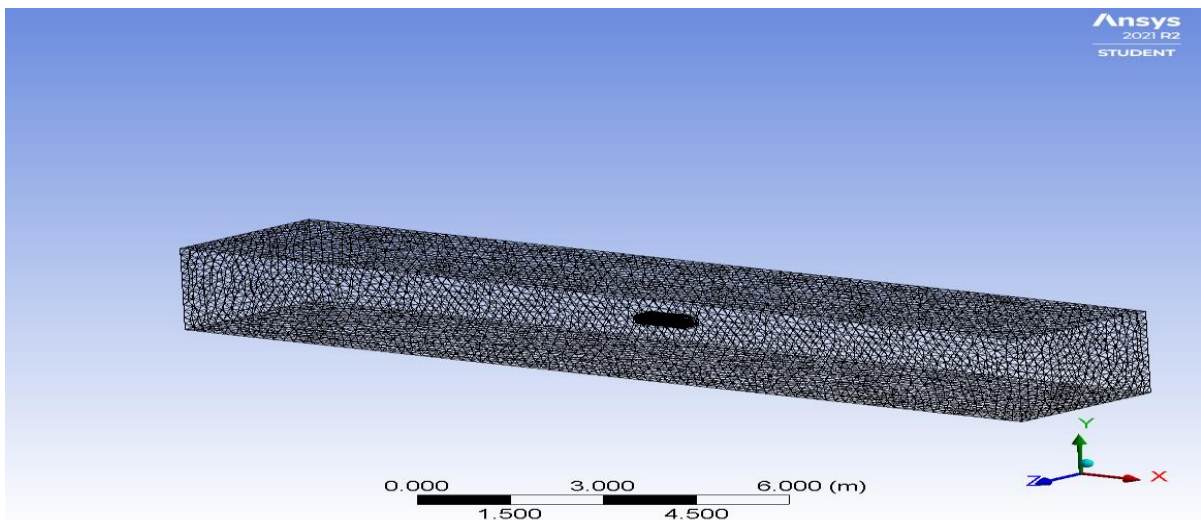


Figure 4.3(iv):- Mesh for Ahmed body

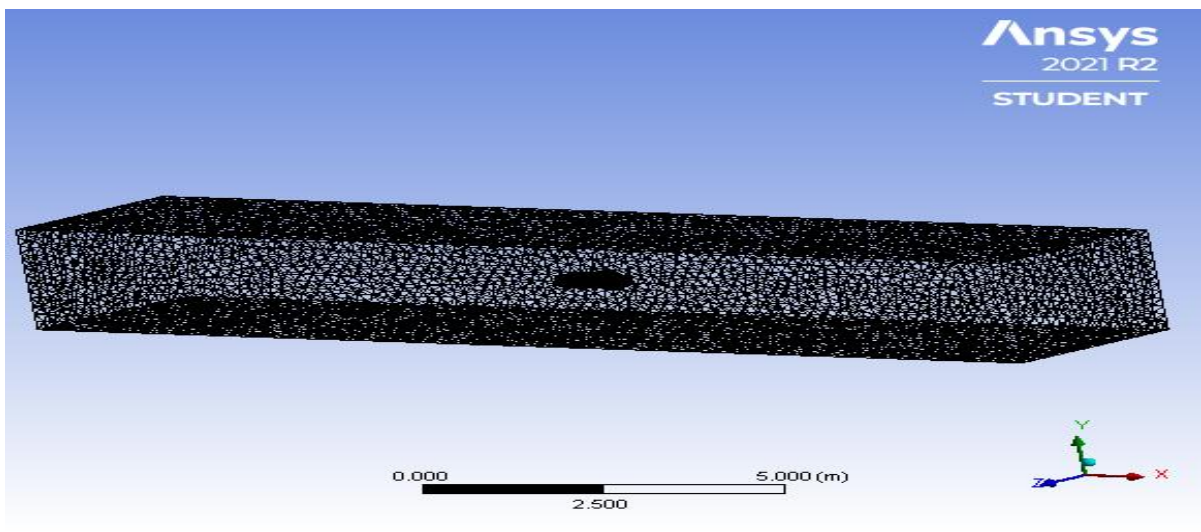


Figure 4.3(v):-Mesh for Ahmed body with blower at its top

Figure 4.3(iv) shows the mesh generated for the designed Ahmed body is shown, where hexahedral meshing is done with number of cells = 71296 , number of faces = 380261, and number of nodes = 276564.

Figure 4.3(v) shows the mesh generated for the designed Ahmed body with blower at its top is shown, where hexahedral meshing is done with number of cells = 86261, number of faces = 445764, and number of nodes = 316237.

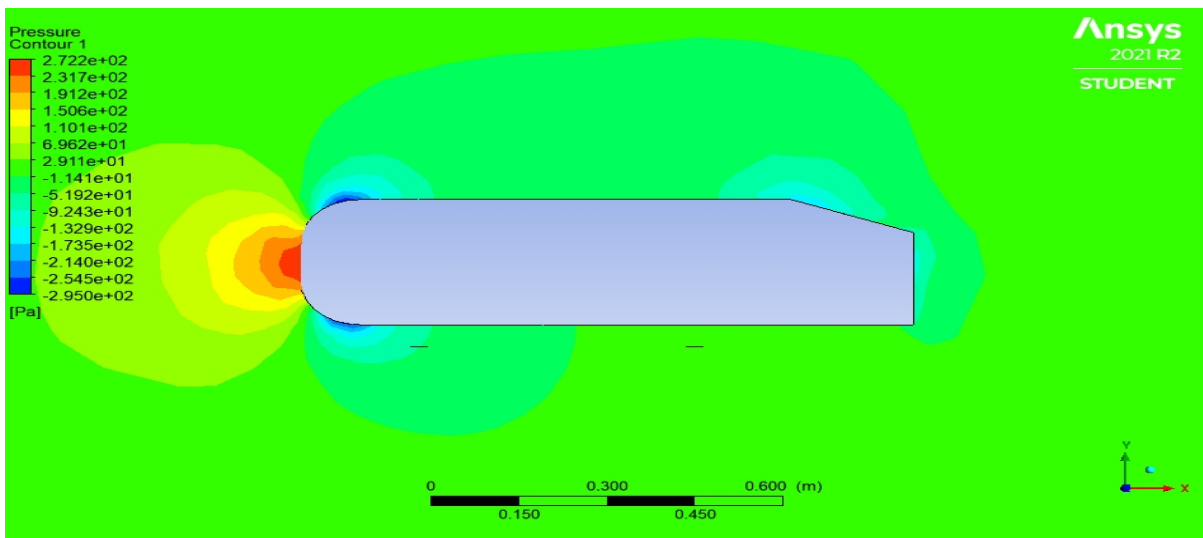


Figure 4.3(vi):- Pressure contour of Ahmed body

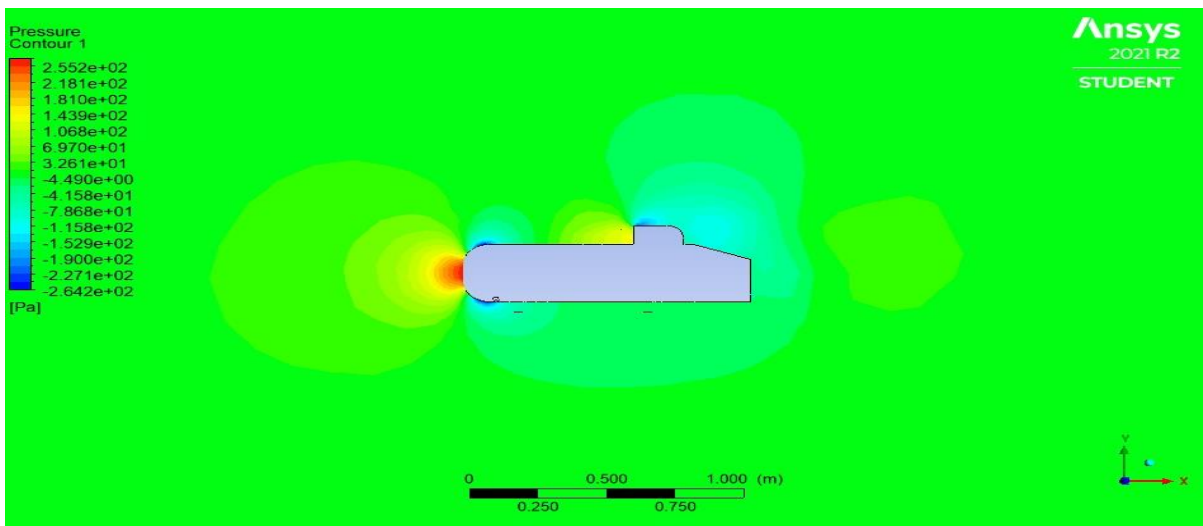


Figure 4.3(vii):-Pressure contour of Ahmed body with blower at its top

The above Figure 4.3(vi) shows the total pressure contour for Ahmed body is shown where minimum obtained total pressure is -295.0 (pa) and maximum pressure obtained is 272.2 (pa).

The above Figure 4.3(vii) shows the total pressure contour for Ahmed body with blower at its top is shown where minimum obtained total pressure is -264.2 (pa) and maximum pressure obtained is 255.2 (pa).

It can be seen that there is additional wake region is generated for body with attached blower at its top, in the rear side, due to attached blower.

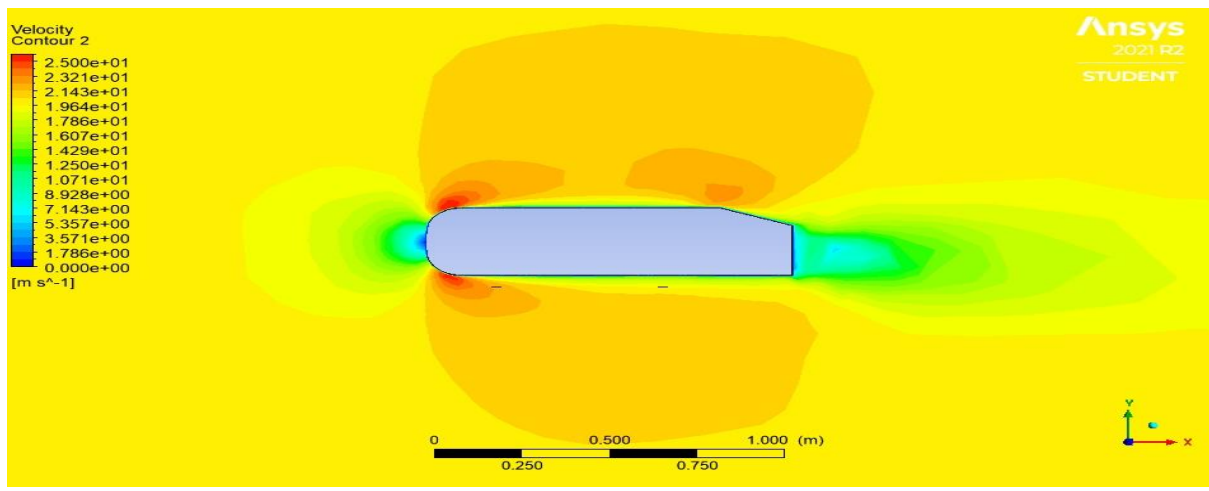


Figure 4.3(viii):- Velocity contour for Ahmed body

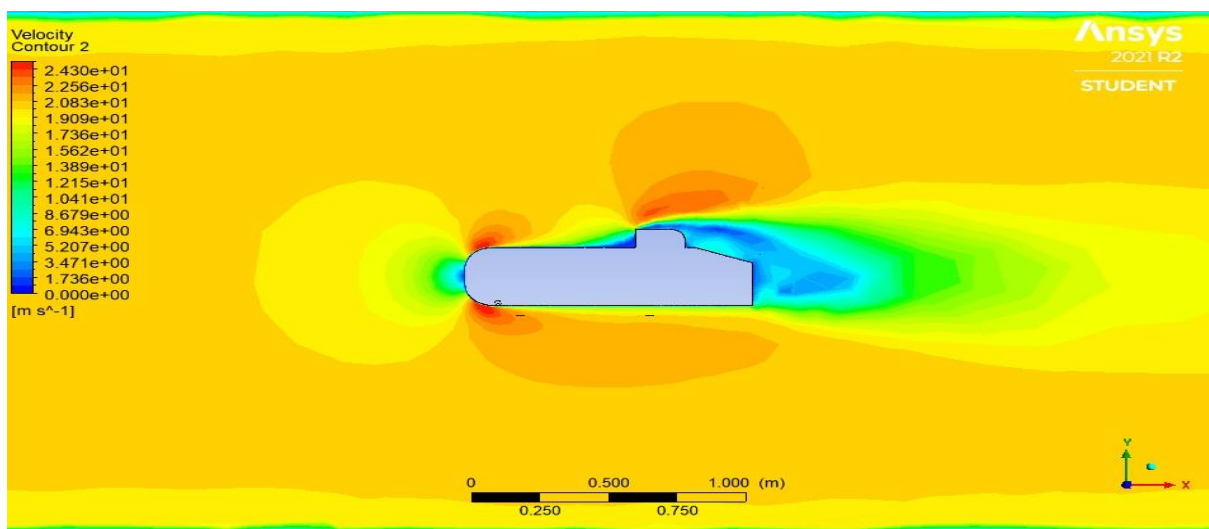


Figure 4.3(ix):-velocity contour for Ahmed body with blower at its top

In the above Figure 4.3(viii), velocity contour for Ahmed body is shown, where the velocity magnitude ranges from 0-25.0 m/s.

In the above Figure 4.3(ix), velocity contour for Ahmed body with blower at its top, where the velocity magnitude ranges from 0-24.3 m/s, which is similar velocity than former case.

Here a substantial decrement in velocity in the rear side for later case can be observed.(in Fig III-i), due to attached blower.

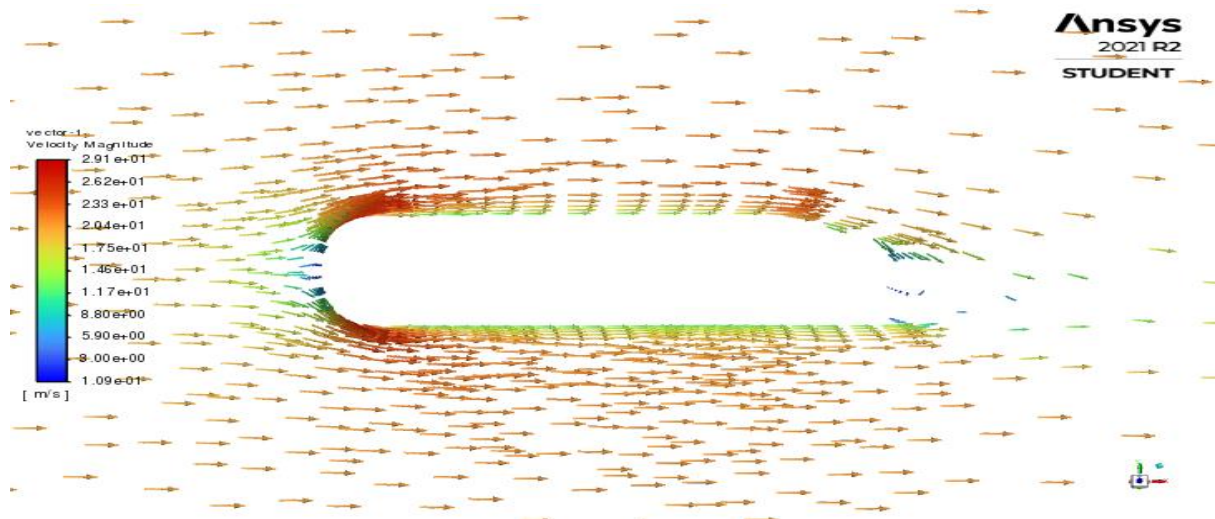


Figure 4.3(x):- Velocity vector for Ahmed body

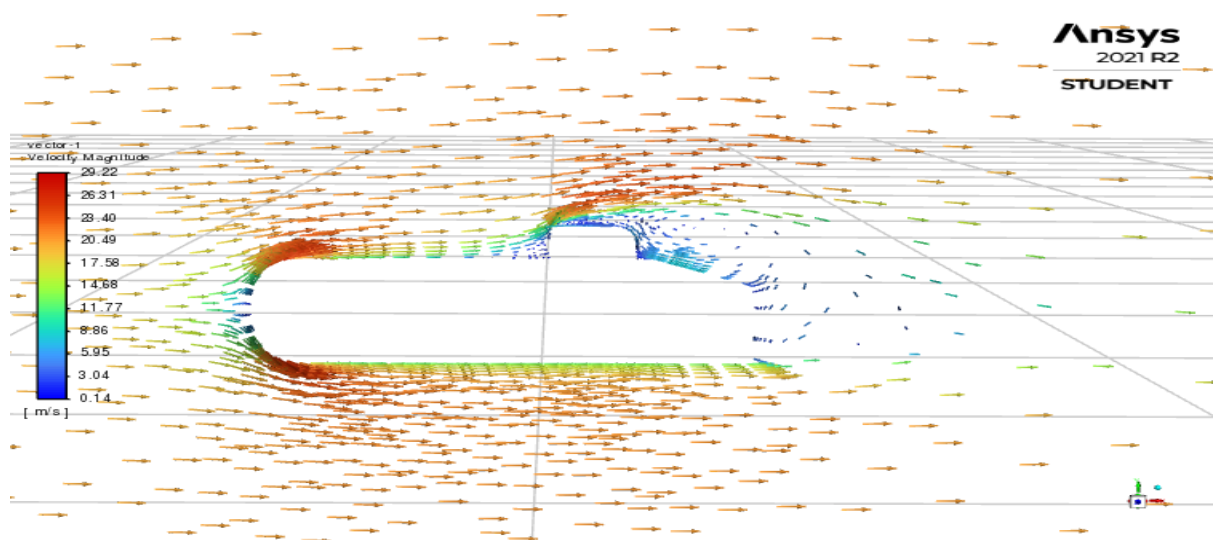


Figure 4.3(xi):-velocity vector for Ahmed body with blower at its top

Ahmed body: -

During meshing, element size = 0.2m, Nodes = 276564, Cells = 71296, Faces = 380261.

$$\text{Projected area } (A_P) = 0.1150138 \text{ m}^2$$

$$\text{Hydraulic Diameter } (D_H) = 4 \cdot A/P$$

$$= 2.87\text{m}$$

During simulation I performed 1000 iterations in which it partially converged and in this I got,

Using this and considering the velocity of vehicle 20m/s(=72km/h) I got the drag coefficient(C_D) value = **0.55** and the drag force(F_D) value = **15.5N**

Ahmed body with blower at the top:-

During meshing, element size = 0.2m, Nodes = 316237, Cells = 86261, Faces = 445764 .

$$\text{Projected area}(A_P) = 0.1503876 \text{ m}^2$$

Enclosure, L= 16m, W=3m, H=2.2m.

$$\text{Hydraulic Diameter } (D_H) = 4 * A/P$$

$$= \mathbf{2.93\text{m}}$$

During simulation I performed 800 iterations in which it get fully converged around 148 iterations and in this I get,

Using this and considering the velocity of vehicle 20m/s(=72km/h) I got the drag coefficient(C_D) = **0.5564** and the drag force(F_D) = **20.5N**.

Power required to overcome this drag force = 20.5*20 = 410 watt.

% change in drag force = **32.26%**

Using wind-power equation,

we know that,

$$P = (1/2) \rho A_s v^3 * N_G * N_B * C_P$$

where, P = Power generated.

ρ = Density of wind.

A_s = Swept Area.

N_G = Generator efficiency

N_B = Gear box efficiency

C_P = Power Coefficient

For ideal condition, (where, $N_G, N_B, C_P = 1$),

$$P = (1/2) \rho A_s v^3$$

Since, **Betz limit = 59.3%** i.e, maximum derivable power.

And , with increase in Area (A_s) of blower blades, more power will be generated, but it is restricted due to maximum size constraint when attached on top of the body, as a subtle increment in overall drag force is observed.

Given dimensions, height of blower considered = 0.070 m,

$$\text{Area of one blower} = (\pi/4) * 70^2 * 10^{-6} \text{ m}^2$$

No of blowers used (as per given width) = 5.

$$\text{Power generated using one blower} = (1/2) * 1.225 * (0.003848451) * (20)^3$$

$$= 1.88574099 \text{ watt.}$$

$$\text{Power available considering Betz limit} = 1.88574099 * 0.593 = 1.1182444 \text{ watt}$$

$$\text{Total power available due to all 5 blowers} = 1.1182444 * 5 = \mathbf{5.591222} \text{ watt.}$$

Since, $F_D \propto$ Projected Area

Hence, power generated with attached blower \ll power lost to overcome induced drag.

5. CONCLUSION AND FUTURE SCOPE OF WORK

5.1 CONCLUSION

- CASE I - From comparisons it can be concluded that if we provide some curvy or say circular edges then the drag coefficient gets reduced just like in these cases as I provided the circular edges in place of sharp edges resulting a reduce in drag coefficient by **39.5%**.
- CASE II - While comparing Ahmed body with open window and closed window condition it was observed that for Ahmed body with open window, obtained drag coefficient is **7.5%** greater than that for closed window condition. Hence, we get higher resisting force for open window. Therefore it is better to drive the vehicle with closed windows for lower energy consumption.
- CASE III - Comparing the obtained values of drag force for Ahmed body without blower and one with a blower attached to the top, it can be concluded that drag force value gets increased by **32.26%** when we attach a blower at the top of the body. Also there is an observable increment in drag coefficient when blower is attached.
- Therefore it is not suggested to attach blower at the top of the vehicle, as a high increment in drag force is observed.
- We should use rounder edge as compared to sharp edge for better aerodynamic design.

5.2 FUTURE SCOPE

The detailed comparative study in this thesis for Ahmed body moving under given design and modified criteria requires further study with applied blunt surfaces and gaps with different chassis designs for different vehicles.

The axial airflow condition is considered for this study, whereas angular inlet airflow conditions can be studied considering the design criteria of the vehicle, so as to obtain further optimized designs for altered wind conditions.

Efficiency of blower and other accessories is to be studied while keeping this study as referring values for axial conditions.

The power generations coupled with other sources of power generation (as solar cells), its effect with drag forces, power consumptions and power generations can be studied.

4. REFERENCES

- [1] Anderson Jr, J.D., Fundamentals of aerodynamics. 5th ed. 2010, New Delhi: Tata McGraw-Hill Education.
- [2] Wang J, Li H, Liu Y, Liu T, Gao H (2018) Aerodynamic research of a racing car based on wind tunnel test and computational fluid dynamics. MATEC Web of Conferences 153:1–5. <https://doi.org/10.1051/matecconf/201815304011>.
- [3] Yang X, Cai Z, Ye Q (2019) Aerodynamics analysis of several typical cars. J Eng Thermophys 28(2):269–275. <https://doi.org/10.1134/S1810232819020085>,
- [4] Altinisik A, Kutukceken E, Umur H (2015) Experimental and numerical aerodynamic analysis of a passenger car: influence of the blockage ratio on drag coefficient. J Fluids Eng, Trans ASME 137(8):1–14. <https://doi.org/10.1115/1.4030183>.
- [5] Sudin MN, Abdullah MA, Shamsuddin SA, Ramli FR, Tahir MM (2014) Review of research on vehicles aerodynamic drag reduction methods. Int J Mech Mechatronics Eng 14(2):35–47.
- [6] Chowdhury H, Loganathan B, Mustary I, Moria H, Alam F (2017) Effect of various deflectors on drag reduction for trucks. Energy Procedia 110(December 2016):561–566. <https://doi.org/10.1016/j.egypro.2017.03.185>.
- [7] John David Anderson. (1997) A History of Aerodynamics. Cambridge: Press Syndicate of the University of Cambridge.
- [8] Hucho WH (1997) Aerodynamics of road vehicles, 4th edition, Society of Automotive Engineers (SAE) International, Warrendale.
- [9] Geropp D, Odenthal HJ (2001) Drag reduction of motor vehicles by active flow control using the Coanda effect. Exp Fluids 28(1):74–85. <https://doi.org/10.1007/s003480050010>.
- [10] E. L Houghton, P.W. Carpenter, Steven H. Collicott, Daniel T. Valiente (2013). Aerodynamics for Engineering Students. Oxford: Butterworth-Heinemann.
- [11] Tamás Lajos. (2002) Basics of vehicle aerodynamics. Budapest University of Technology and Economics. Department of Fluid Mechanics.
- [12] Motor 16. Mercedes CLA: el coche más aerodinámico del mundo <http://www.libertaddigital.com/deportes/motor/2013-01-18/mercedes-cla-el-coche-mas-aerodinamico-del-mundo-1276479768/>

- [13] Bosch Inc. (2011). *Bosch Automotive Handbook*: Bentley Publishers
- [14] Obidi, T.Y., Theory and applications of aerodynamics for ground vehicles. 2014: Society of Automotive Engineers.
- [15] Krishnani, P.N., CFD study of drag reduction of a generic sport utility vehicle. 2009, American Society of Mechanical Engineers.
- [16] Schuetz, T., Aerodynamics of road vehicles. Vol. Fifth Edition 2016, USA: Society of Automotive Engineers.
- [17] Reddy Gondipalle, S., CFD Analysis of the Under Hood of A Car for Packaging Considerations. 2011.
- [18] Hilliard, J.C. and G.S. Springer, Fuel Economy: In Road Vehicles Powered by Spark Ignition Engines. 2013: Springer Science & Business Media.
- [19] Heisler, H., Advanced vehicle technology. 2nd Edition ed. 2002, Great Britain Butterworth Heinemann Books - Elsevier.
- [20] Katz, J., Automotive aerodynamics. 2016, Chichester, UK; Hoboken, NJ: John Wiley & Sons.
- [21] Levin, J. and R. Rigdal, Aerodynamic analysis of drag reduction devices on the underbody for SAAB 9-3 by using CFD. Chalmers University of Technology, 2011.
- [22] Hucho, W.-H., Aerodynamics of road vehicles: from fluid mechanics to vehicle engineering. 4th ed. 1998, Warrendale, PA: Society of Automotive Engineers.
- [23] Hucho, W.-H. and S.R. Ahmed, Aerodynamics of road vehicles: from fluid mechanics to vehicle engineering. 1987, London: Butterworths.
- [24] Lay, W., Is 50 Miles Per Gallon Possible With Correct Streamlining?, Part 1. 1933, SAE Technical Paper. 330041, doi:10.4271/330041
- [25] Ahmed, S.R., G. Ramm, and G. Faltin, Some salient features of the time- averaged ground vehicle wake. 1984, SAE Technical Paper.
- [26] Han, T., Computational analysis of three-dimensional turbulent flow around a bluff body in ground proximity. Momentum, 1989. 510: p. 3.

- [27] Minguéz, M., R. Pasquetti, and E. Serre, High-order large-eddy simulation of flow over the “Ahmed body” car model. *Physics of fluids*, 2008. 20(9): p. 095101.
- [28] Bello-Millán, F., et al., Experimental study on Ahmed's body drag coefficient for different yaw angles. *Journal of Wind Engineering and Industrial Aerodynamics*, 2016. 157: p. 140-144.
- [29] Guilmineau, E., Computational study of flow around a simplified car body. *Journal of wind engineering and industrial aerodynamics*, 2008. 96(6): p. 1207- 1217.
- [30] Conan, B., J. Anthoine, and P. Planquart, Experimental aerodynamic study of a car-type bluff body. *Experiments in Fluids*, 2011. 50(5): p. 1273-1284.
- [31] Howard, R. and M. Pourquie, Large eddy simulation of an Ahmed reference model. *Journal of Turbulence*, 2002. 3(5).
- [32] Hinterberger, C., M. Garcia-Villalba, and W. Rodi, Large eddy simulation of flow around the Ahmed body, in *The aerodynamics of heavy vehicles: trucks, buses, and trains*. 2004, Springer. p. 77-87.
- [33] KrajnoviÄ, S.a. and L. Davidson, Flow around a simplified car, part 1: large eddy simulation. *Journal of Fluids Engineering*, 2005. 127(5): p. 907-918.
- [34] Serre, E., et al., On simulating the turbulent flow around the Ahmed body: A French–German collaborative evaluation of LES and DES. *Computers & Fluids*, 2013. 78: p. 10-23.
- [35] Verzicco, R., et al., Large eddy simulation of a road vehicle with drag-reduction devices. *AIAA journal*, 2002. 40(12): p. 2447-2455.
- [36] Franck, G., et al., Numerical simulation of the flow around the Ahmed vehicle model. *Latin American applied research*, 2009. 39(4): p. 295-306.
- [37] Watkins, S. and G. Vio, The effect of vehicle spacing on the aerodynamics of a representative car shape. *Journal of wind engineering and industrial aerodynamics*, 2008. 96(6): p. 1232-1239.
- [38] Meile, W., et al., Experiments and numerical simulations on the aerodynamics of the Ahmed body. *CFD Letters*, 2011. 3(1): p. 32-39.

- [39] Thacker, A., et al., Effects of suppressing the 3D separation on the rear slant on the flow structures around an Ahmed body. *Journal of Wind Engineering and Industrial Aerodynamics*, 2012. 107: p. 237-243.
- [40] Ortega, J., et al., Aerodynamic drag reduction of class 8 heavy vehicles: a full-scale wind tunnel study. 2013, Lawrence Livermore National Laboratory (LLNL), Livermore, CA.
- [41] Hilmi Safuan, J., *Aerodynamic Study Of Heavy Truck Using CFD Fluent*. 2010.
- [42] Gilkeson, C., et al., An experimental and computational study of the aerodynamic and passive ventilation characteristics of small livestock trailers. *Journal of Wind Engineering and Industrial Aerodynamics*, 2009. 97(9-10): p. 415-425.
- [43] Guo, L., Y.-M. Zhang, and W.-J. Shen, Simulation Analysis of Aerodynamics Characteristics of Different Two-Dimensional Automobile Shapes. *JCP*, 2011. 6(5): p. 999-1005.
- [44] Harinaldi, H., et al., Modification of flow structure over a van model by suction flow control to reduce aerodynamics drag. *Makara Journal of Technology*, 2012. 16(1): p. 15-21.
- [45] Altinisik, A., E. Kutukceken, and H. Umur, Experimental and Numerical Aerodynamic Analysis of a Passenger Car: Influence of the Blockage Ratio on Drag Coefficient. *Journal of Fluids Engineering-Transactions of the ASME*, 2015. 137(8): p. 81104.
- [46] Tsubokura, M., et al., Large eddy simulation on the unsteady aerodynamic response of a road vehicle in transient crosswinds. *International Journal of Heat and Fluid Flow*, 2010. 31(6): p. 1075-1086.
- [47] Sealy, M., et al., *Motor coach*. 1996, Google Patents: USA.
- [48] Roy, S. and P. Srinivasan, External flow analysis of a truck for drag reduction. 2000, SAE Technical Paper. 2000-01-3500, <https://doi.org/10.4271/2000-01-3500>.
- [49] Amirnordin, S.H., et al., Numerical analysis on the effects of air flow in the wake of a large vehicle on trailing a passenger car. *Malaysian Technical Universities Conference on Engineering and Technology (MUCET)*, 2010.

- [50] Ghani, O.A., Design optimization of aerodynamic drag at the rear of generic passenger cars using nurbs representation, in Mechanical Engineering. 2013, University of Ontario: UOIT.
- [51] Hucho, W.-h. and G. Sovran, Aerodynamics of road vehicles. Annual review of fluid mechanics, 1993. 25(1): p. 485-537.
- [52] Rossitto, G., et al., Influence of afterbody rounding on the pressure distribution over a fastback vehicle. Experiments in Fluids, 2016. 57(3): p. 43.
- [53] Miralbes, R. Analysis of Some Aerodynamic Improvements for Semi-Trailer Tankers. in Proceedings of the World Congress on Engineering. 2012.
- [54] Barbut, D. and E.M. Negrus, CFD analysis for road vehicles-case study. INCAS bulletin, 2011. 3: p. 15-22.
- [55] Song, K.-S., et al., Aerodynamic design optimization of rear body shapes of a sedan for drag reduction. International Journal of Automotive Technology, 2012. 13(6): p. 905-914.
- [56] Khalighi, B., K.-H. Chen, and G. Iaccarino, Unsteady aerodynamic flow investigation around a simplified square-back road vehicle with drag reduction devices. Journal of fluids engineering, 2012. 134(6): p. 061101.
- [57] Du Buisson, J. and J. Erens, Reduction of Aerodynamic Resistance of Heavy Vehicles and Effect on Fuel Economy. 1990.
- [58] Leuschen, J. and K.R. Cooper, Full-scale wind tunnel tests of production and prototype, second-generation aerodynamic drag-reducing devices for tractor- trailers. 2006, SAE Technical Paper. 2006-01-3456, <https://doi.org/10.4271/2006-01-3456>.
- [59] Van Raemdonck, G.M. and M.J. Van Tooren. Design of an aerodynamic aid for the underbody of a trailer within a tractor-trailer combination. in BBAA VI International Colloquium on Bluff Bodies Aerodynamics & Applications Milano, Italy. 2008.
- [60] Salari, K. and J. Ortega, Aerodynamic Design Criteria for Class 8 Heavy Vehicles Trailer Base Devices to Attain Optimum Performance. 2010, Lawrence Livermore National Laboratory (LLNL), Livermore, CA.

- [61] Farkas, S., Fuel Efficiency in Truck Industry. Scientific Bulletin of the "Petru Maior" University of Targu Mures, 2010. 7(2): p. 59.
- [62] Shukri, I. and A. Akram. Improvement of aerodynamics characteristic of heavy trucks. in 3rd International Conference on Trends in Mechanical and Industrial Engineering (ICTMIE'2013) January. 2013.
- [63] Chowdhury, H., et al., A study on aerodynamic drag of a semi-trailer truck. Procedia Engineering, 2013. 56: p. 201-205.
- [64] CFD Online. *Standard K-epsilon model* http://www.cfd-online.com/Wiki/Standard_k-epsilon_model